water

MDPI

Article

Hydrological Dynamics of Raipur, Chhattisgarh in India: Surface–Groundwater Interaction Amidst Urbanization

Dalchand Jhariya [1,*], Mayank Shrivastav [1], Rajendrakumar D. Deshpande [2] and Virendra Padhya [2]

[1] Department of Applied Geology, National Institute of Technology Raipur, Raipur 492010, India; mshrivastav.jrf2022@nitrr.ac.in
[2] Geoscience Division, Physical Research Laboratory, Ahmedabad 380009, India; desh@prl.res.in (R.D.D.); virendra@prl.res.in (V.P.)
* Correspondence: dcjhariya.geo@nitrr.ac.in

Abstract: The hydrological dynamics of Raipur are profoundly influenced by the intricate interplay between surface and groundwater systems, driven by changes in land use, climatic conditions, and human activities such as agriculture and industry. This research investigated the interdependencies between the Kharun River and groundwater systems, essential for understanding water security in the face of escalating demands and rapid urbanization. Through meticulous monitoring and analysis of approximately 70 bore wells, nine river sampling sites, and 13 groundwater samples from dug wells, alongside rigorous adherence to established sampling protocols, this study delved into the seasonal variations and influences on water quantity and quality. Statistical methodologies, stable isotope analyses, and Gibbs diagrams were employed to unravel the complexities governing water resource dynamics and interactions. Notably, correlation analysis revealed significant associations between various water quality parameters, indicating anthropogenic influences on groundwater chemistry. Cluster analysis aided in understanding hydro-chemical processes, while stable isotope examinations further elucidated the sources and interactions of groundwater and surface water. Results indicate the urgent need for sustainable water management strategies tailored to the region's evolving socio-environmental landscape, considering escalating urbanization and agricultural activities. This integrated approach, combining analytical methods and statistical techniques, offers a holistic understanding of water resource dynamics essential for effective governance and sustainable development.

Keywords: hydrological dynamics; interactions; groundwater chemistry; urbanization impacts; water security; stable isotope analysis; anthropogenic influences; sustainable water management

check for updates

Academic Editor: Mohamad Basel Al Sawaf

Received: 5 February 2025
Revised: 13 March 2025
Accepted: 19 March 2025
Published: 22 March 2025

Citation: Jhariya, D.; Shrivastav, M.; Deshpande, R.D.; Padhya, V. Hydrological Dynamics of Raipur, Chhattisgarh in India: Surface–Groundwater Interaction Amidst Urbanization. *Water* **2025**, *17*, 930. https://doi.org/10.3390/w17070930

Copyright: © 2025 by the authors. Licensee MDPI, Basel, Switzerland. This article is an open access article distributed under the terms and conditions of the Creative Commons Attribution (CC BY) license (https://creativecommons.org/licenses/by/4.0/).

1. Introduction

The intricate relationship between surface and groundwater holds paramount importance within Raipur's hydrological dynamics, where it is significantly influenced by shifts in land use patterns, alterations in climate conditions, and various anthropogenic activities such as agricultural and industrial practices. The process of urbanization, particularly evident along the course of the Kharun River following Raipur's designation as the capital of Chhattisgarh in 2000, has notably escalated the extraction of groundwater resources to fulfil burgeoning societal needs. However, this heightened demand, coupled with inadequate management strategies and unsustainable utilization practices, poses a substantial threat to the availability of potable water sources within the region. Furthermore, the intricate interplay between river dynamics and groundwater underscores the necessity

for meticulous surveillance aimed at preserving both the quantity and quality of water resources. Given the escalating pressures on water availability due to rapid population growth, a comprehensive understanding of the seasonal dependencies between the Kharun River and groundwater systems emerges as imperative for ensuring water security in Raipur. Addressing the challenges of water scarcity necessitates the implementation of enduring solutions tailored to the region's evolving socio-environmental landscape.

Overview of the Study Area

The catchment area of the Kharun River, as represented in Figure 1, plays a vital role in the urban development of Raipur, primarily relying on groundwater extraction from aquifers to meet public water demands. The interconnectedness between rainwater, groundwater, and surface water highlights their mutual reliance. Despite consistent rainfall patterns, increasing water consumption has led to unpredictable fluctuations in both water levels and quality. The rapid urbanization witnessed in Raipur is anticipated to further aggravate the depletion of groundwater resources. It is imperative to conduct thorough investigations into the factors influencing groundwater quantity and quality, the reciprocal relationship between the Kharun River and adjacent aquifers, and seasonal variations. Sustainable management of water resources has become crucial in light of the growing population and agricultural activities. The study area, located within the Seonath sub-basin of the Mahanadi River basin in Chhattisgarh, encompasses the Kharun watershed, where Raipur's tropical climate and dense population heavily rely on both groundwater and the river. Urgent measures are necessary to address the pressing issues of water scarcity and diminishing groundwater levels resulting from intensified urbanization. Effective solutions require comprehensive, long-term planning strategies.

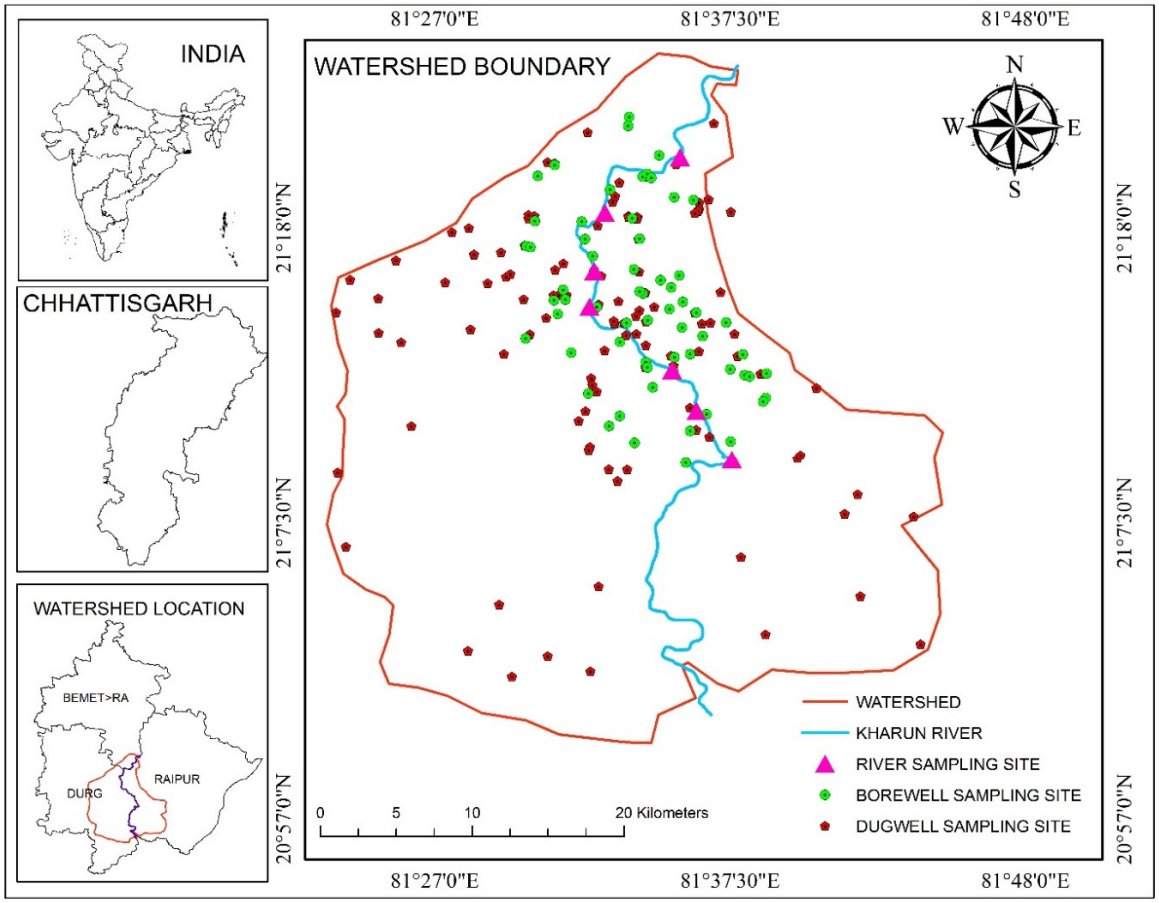


Figure 1. Study area map.

2. Literature Review

Urban expansion globally poses significant challenges for water quality and quantity [1–10].

Urbanization along rivers exacerbates problems due to their interaction with groundwater and surface water [11–15].

Understanding this interaction involves characterizing surface water bodies regarding water exchange with groundwater, seasonal variations, and extraction rates [16–24]

Globally, research emphasizes urban water resource management and surface water-groundwater interactions [25–27]. Specific impacts of urban development on water resources are well-documented.

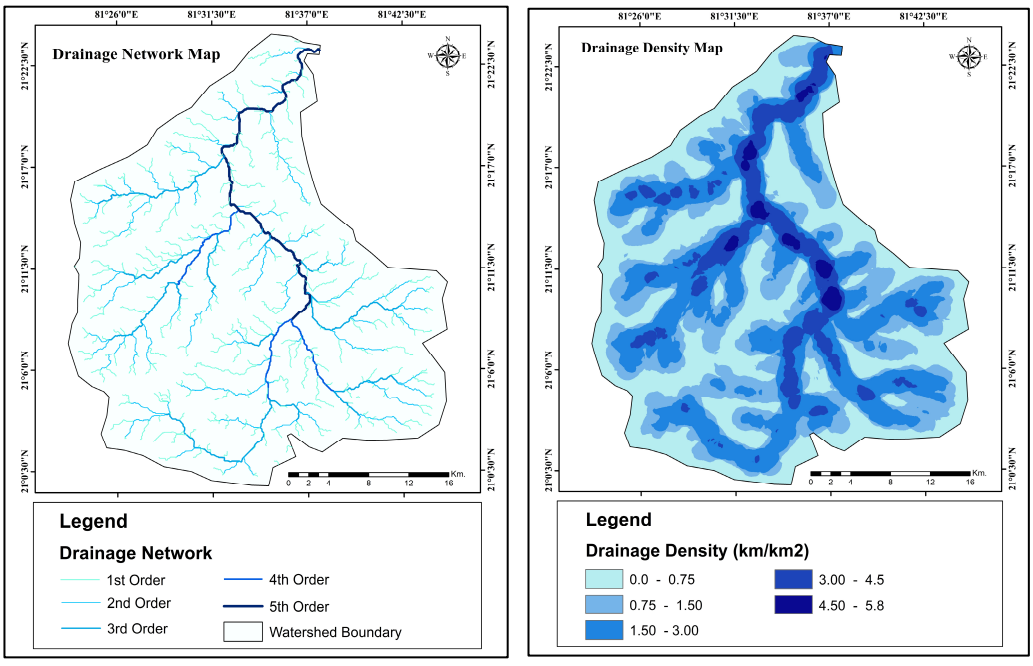
Agricultural regions witness dwindling groundwater levels, intensifying water scarcity [28,29]. Groundwater quality and quantity are affected by surface-water interactions across India [17,30–32].

Sustainable urbanization in water-stressed areas requires integrated measures such as inter-city water networks and eco-friendly urban planning [33–43].

3. Materials and Methods

Various thematic layers were generated, including geology, geomorphology, drainage, slope, groundwater table, and land use/land cover, employing ArcGIS software (Arcmap) to identify artificial recharge zones within the study area.

The creation of drainage maps and drainage density maps utilized Survey of India (SOI) topo sheets and Sentinel-2 imagery through ArcGIS software (Arcmap). It can be observed from the drainage network map, as shown in Figure 2, that there are five orders, and it can be inferred from the drainage density map that the density varies from 0 to 5.8 Km/Km^2.



(**a**) (**b**)

Figure 2. Drainage structure map: (**a**). drainage network map; (**b**). drainage density map.

Geomorphological features such as pediments, floodplains, hills, and plains play a crucial role in groundwater studies, as shown in Figure 3. The geomorphological map

was created through visual interpretation using data from the Geological Survey of India's Bhukosh portal.

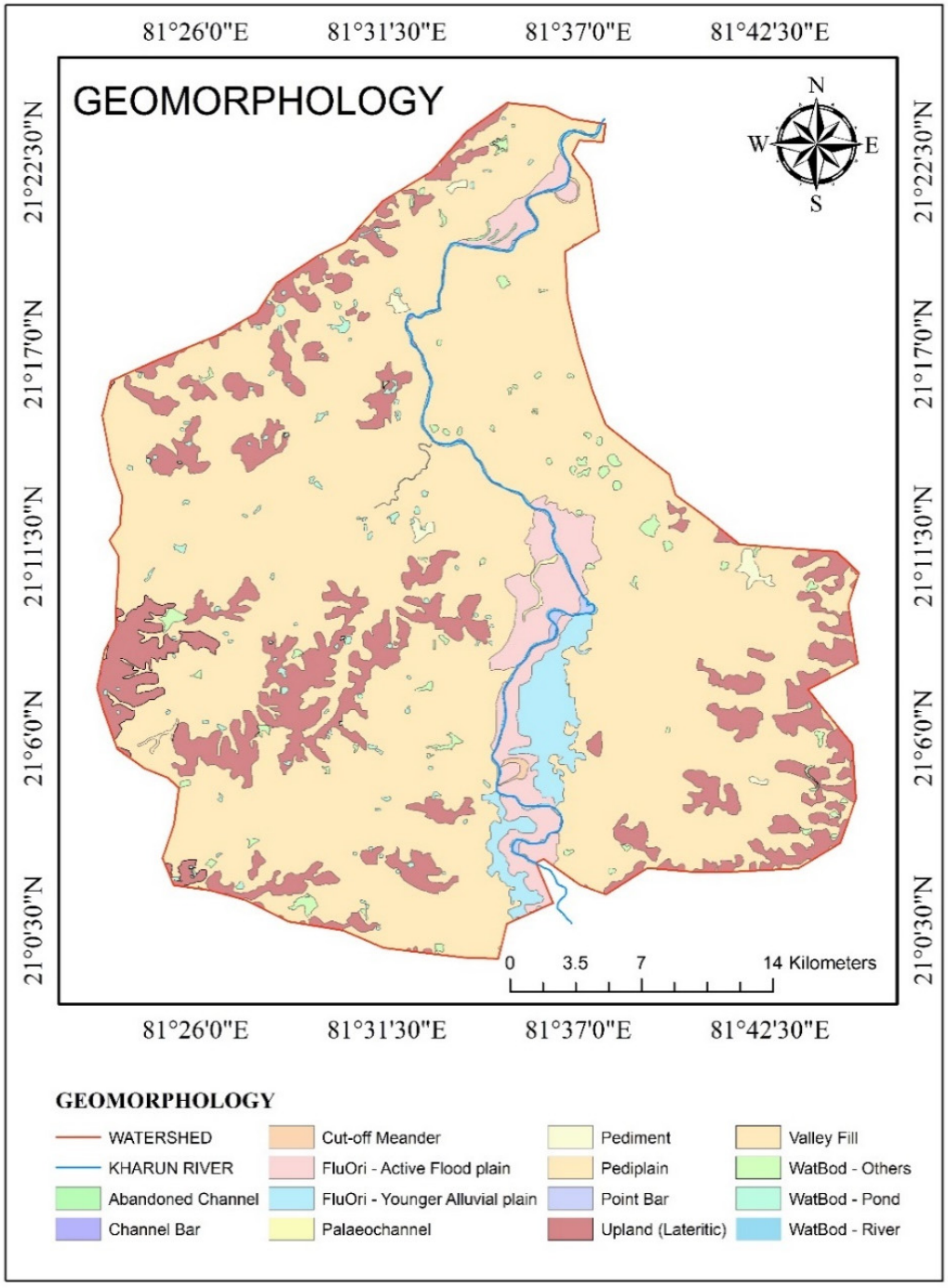


Figure 3. Geomorphologic map of the study area.

The presence and dynamics of groundwater are intricately linked to the geological context. The geological map, as shown in Figure 4, was developed through visual interpretation using data extracted from the Bhukosh portal of the Geological Survey of India, in conjunction with GIS software. The geological map indicates that Stromatolitic Dolomitic Limestone predominantly covers the study area, with other geological formations present in smaller proportions.

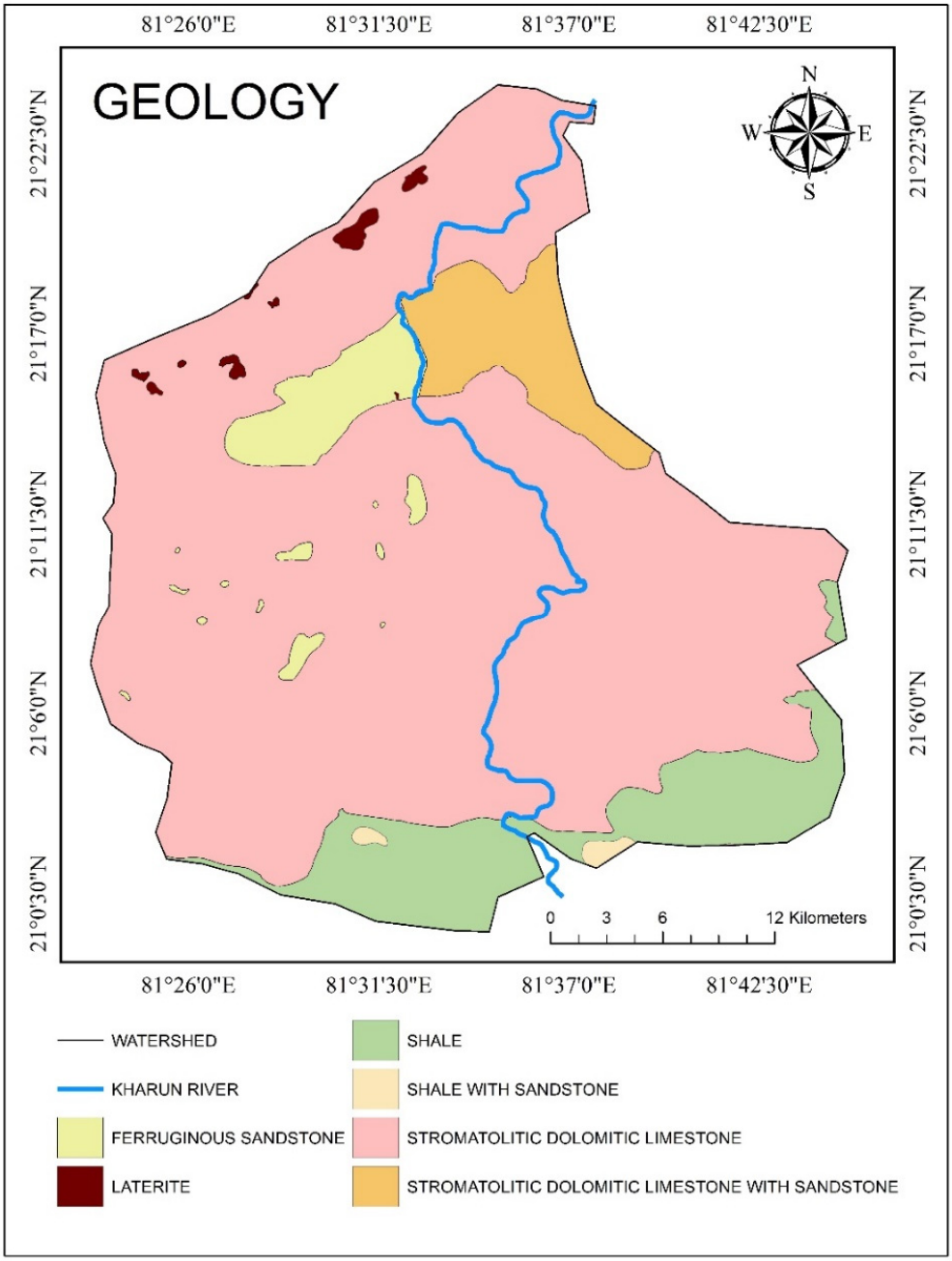


Figure 4. Geological map of the study area.

The slope map, as shown in Figure 5, influences the rate of water infiltration, with steeper gradients leading to increased runoff and a reduced capacity for groundwater retentio. In contrast, milder slopes offer enhanced potential for groundwater storage by mitigating runoff. The generation of the slope map entailed the application of Survey of India (SOI) toposheets and Digital Elevation Models (DEMs) within ArcGIS software. It can be inferred from the below figure that the slope varies from 0 to 67.74%.

The alteration of land use and land cover within a region plays a crucial role in determining the quality of both surface water and groundwater. Modifications in the placement and scale of potential sources of groundwater contamination can exert a substantial impact on groundwater quality. In the present study, we used the Living Atlas websites of ESRI to prepare the LULC change map for the years 2017 to 2022, as shown in Figure 6.

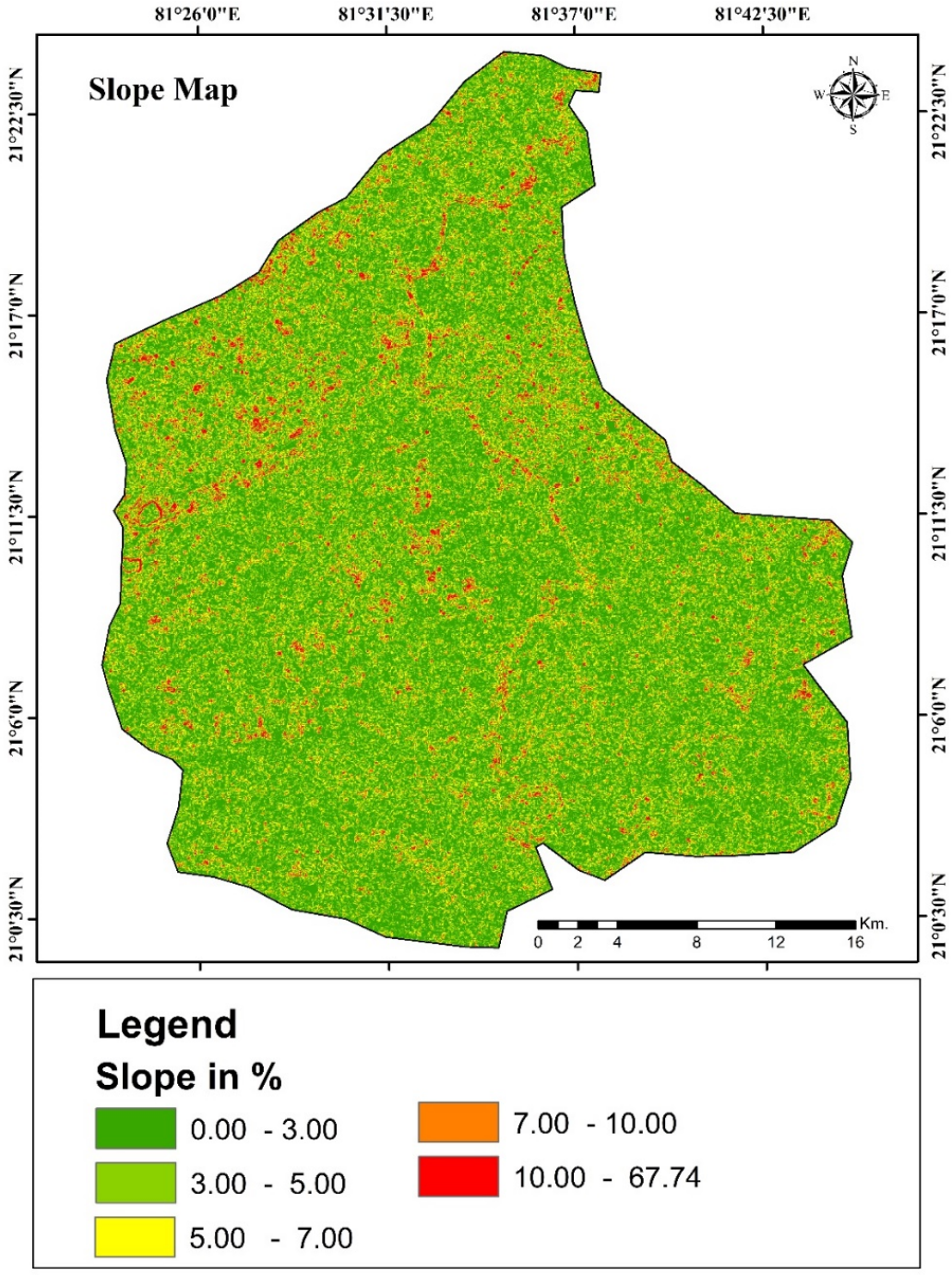


Figure 5. Slope map of the study area.

The study of land cover classes from 2017 to 2022 revealed notable trends, as indicated by the percentage of area coverage for each category, as shown in Figure 7. In 2017, water bodies comprised 2.40% of the total area, with trees covering 0.96%, flooded vegetation accounting for 0.12%, crops occupying 67.89%, built areas constituting 13.76%, and both bare ground and range land each comprising 14.83%. Subsequent years saw fluctuations in coverage percentages for each land cover class. Notably, water bodies experienced slight variations, ranging from 2.04% in 2018 to 2.67% in 2022. Trees exhibited a decrease from 0.44% in 2018 to 0.84% in 2022, while flooded vegetation maintained consistently low percentages throughout the years. Crops remained a predominant land cover class, with coverage percentages ranging from 68.09% in 2022 to 74.87% in 2021. Built areas demonstrated a consistent increase from 13.76% in 2017 to 16.91% in 2022. Additionally,

both bare ground and range land experienced fluctuations in coverage percentages over the specified years.

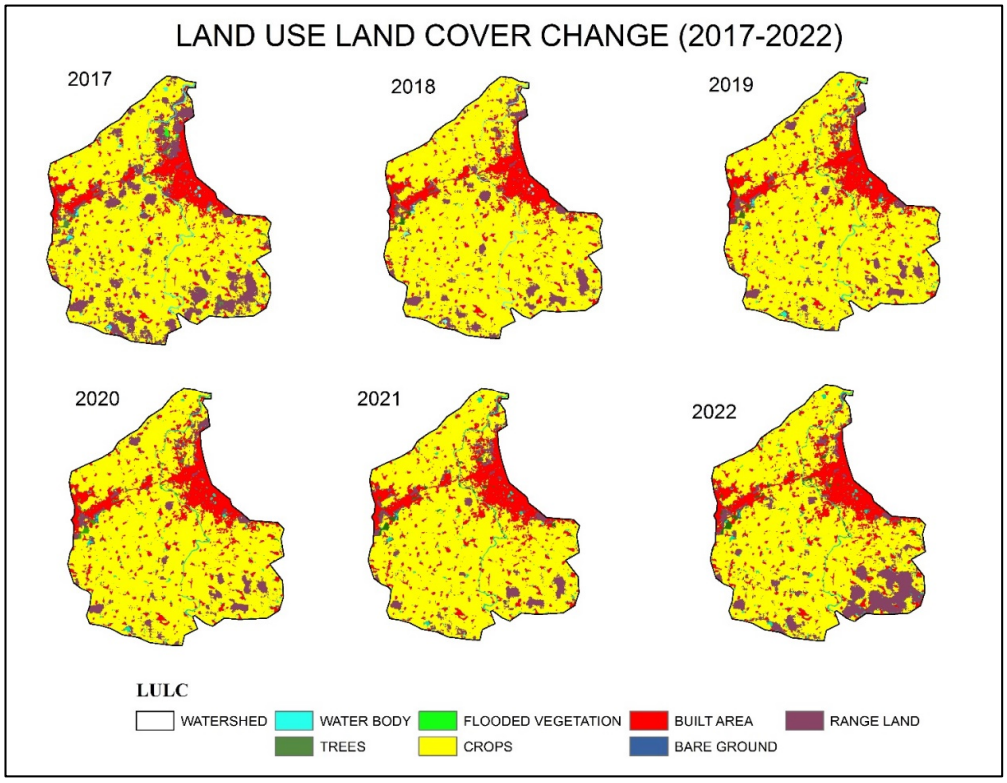


Figure 6. Land use land cover (LULC) map of the study area.

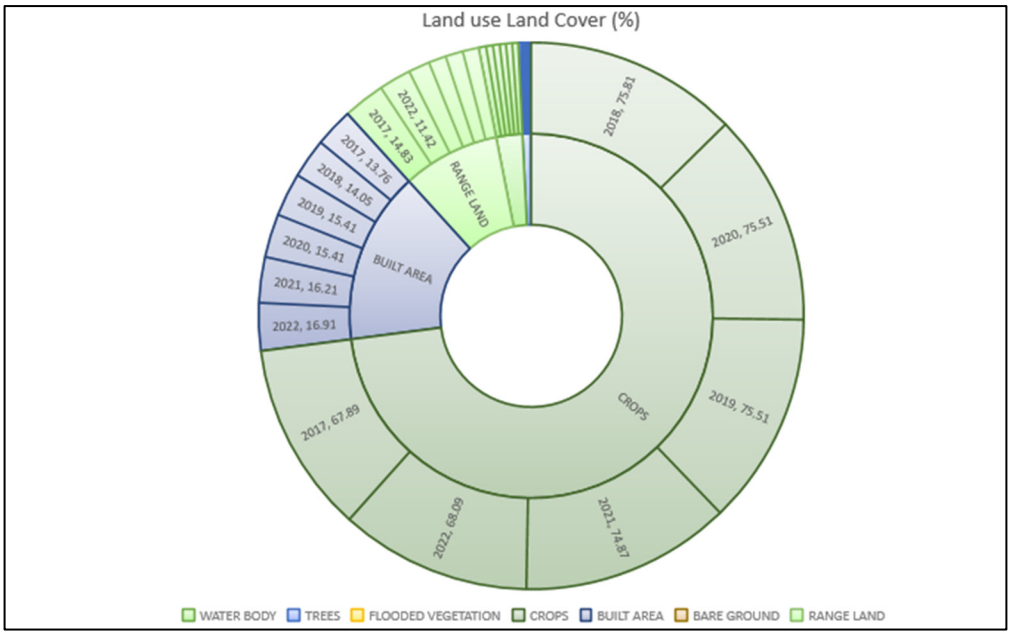


Figure 7. Graphical representation of land use land cover change.

3.1. Groundwater Quality Study

A total of approximately 70 bore wells representative of the region, along with nine sampling sites along the river and 13 groundwater samples from dug wells, were strategically selected for regular monitoring purposes. Groundwater and surface water samples were acquired following established protocols outlined by the American Public Health Association (APHA), encompassing both pre-monsoon and post-monsoon periods. To ensure the accuracy of sample collection, meticulous cleaning procedures were followed for the sample bottles, involving a sequence of concentrated hydrochloric acid (HCl), tap water, and distilled water rinsing. Moreover, at the sampling sites, measures were taken to minimize contamination by rinsing the sample bottles with the specific water source intended for sampling. Each sampling location yielded distinct samples, which were then preserved in high-density polyethene (HDPE) containers for subsequent analysis. In the context of this particular investigation, samples from all locations were collected in two separate containers: one container was treated with a 5% nitric acid (HNO_3) solution to maintain the metals in a dissolved state for trace contaminants and heavy metal analysis, while the other container remained devoid of any added preservatives. Furthermore, as part of the water sampling procedure, field parameters such as electrical conductivity (EC), temperature (T), and hydrogen-ion concentration (pH) were measured on-site using a field analyzer. The geographical coordinates of the sampling locations were accurately recorded with the aid of a handheld GPS device.

In the current study, the primary parameters under investigation encompassed the quantification of various chemical and physical attributes. These attributes included the determination of pH (hydrogen-ion concentration), EC (electrical conductivity), T (temperature), TH (total hardness), Ca (Calcium), Mg (Magnesium), Na (Sodium), K (Potassium), HCO_3 (hydrogen carbonate), Cl (chloride), NO_3 (nitrate), SO_4 (sulphate), F (fluoride), Fe (Iron), and TDS (total dissolved solids). The methodologies employed for these measurements adhered to the established procedures delineated in the standard operating protocols prescribed by the 23rd Edition of the American Public Health Association (APHA) manual.

3.2. Groundwater and Surface Water Assessment

An all-encompassing strategy was deployed to explore the intricate interconnection between groundwater and surface water, utilizing a diverse array of analytical methods. These included examinations of rock–water interactions, statistical methodologies, and stable isotope analyses. This integrated approach aimed to unravel the complexities governing the interaction dynamics, thus yielding valuable insights into hydrological systems and their governance. By amalgamating these varied analytical techniques, the study endeavored to provide a holistic evaluation of the interplay among geological, hydrological, and environmental factors influencing water resource dynamics. Such a multidisciplinary strategy not only amplifies the credibility of the findings but also propels advancements in the realm of hydrology and water resource management.

3.3. Stable Isotope Analysis

Diverse water samples were obtained from both surface water and groundwater reservoirs for the purpose of stable isotope examination. The collection of precipitation samples occurred during the southwest monsoon season, encompassing both the study area and neighboring regions, with the objective of establishing a Local Meteoritic Water Line (LMWL). Given the prevalent occurrence of rainfall during the southwest monsoon, meticulous collection of rainwater samples was ensured to coincide with this temporal pattern. To mitigate the risk of potential contamination, unfiltered samples were meticulously acquired in 250 mL high-density polyethene (HDPE) containers and meticulously labelled on-site.

Following collection, these samples were transported to the Geosciences Division of the Physical Research Laboratory (PRL) in Ahmedabad, India for subsequent analysis of stable water isotopes. The stable oxygen and hydrogen isotope ratios were determined through the standard gas equilibration method employing an isotope ratio mass spectrometer (Delta V plus, Thermo Scientific, 168 Third Avenue, Waltham, MA, USA).

4. Results and Discussion

4.1. Ground Water Table (GWT) Study

The depth of the groundwater table is governed by the dynamic interaction between recharge and discharge processes within the groundwater system. In this study, groundwater levels were monitored at multiple locations across the study area, and the collected data were utilized to generate a groundwater table map using GIS software. Spatial interpolation using IDW was applied to visualize the distribution of groundwater levels, revealing consistent patterns of extreme highs and lows across different plots, as shown in Figure 8. These extremes may be attributed to localized geological formations, variations in land use, or differences in recharge and discharge rates, necessitating further investigation. Moreover, seasonal variations were evident, with groundwater levels ranging from 203.35 masl to 391.3 masl in the pre-monsoon season and from 204 masl to 391.6 masl in the post-monsoon season, with an average fluctuation of 0.81216 masl. These fluctuations indicate a slight overall rise in the groundwater table following the monsoon, likely due to increased recharge from rainfall. Understanding these seasonal variations is essential for effective water resource management, particularly in ensuring sustainable groundwater utilization and mitigating the risks associated with water scarcity.

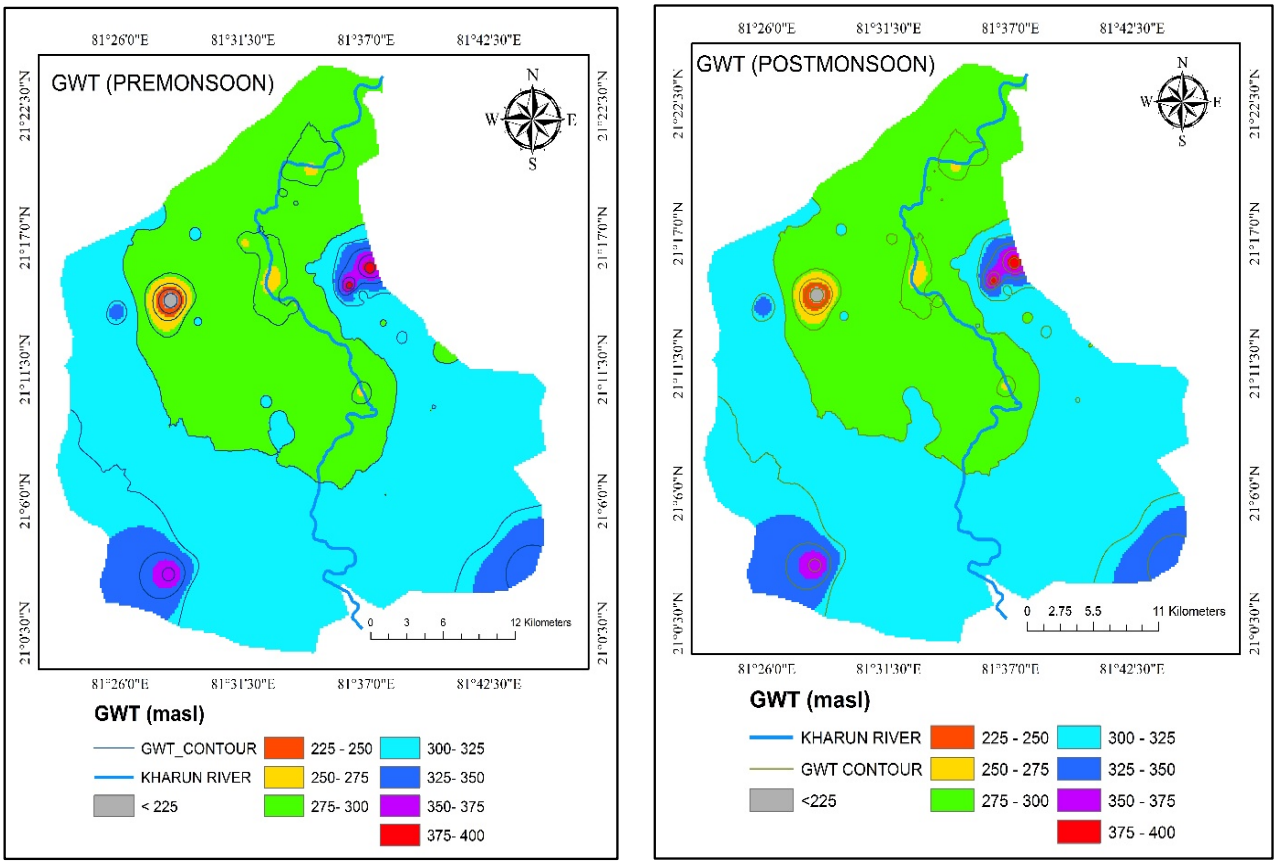


Figure 8. Ground water table (GWT) map.

4.2. Groundwater and Surface Water Type

The groundwater within the study area is generally colorless, with the exception of a few samples exhibiting a light orange hue. It is characterized as odorless and possessing a favorable taste. Depending upon the season, groundwater has a temperature different from the surface temperature of the atmosphere. The results show that, during the pre-monsoon phase, groundwater has $Na^+ > Ca^{2+} > Mg^{2+} > K$ and $Cl^- > HCO_3 > SO_4^{2-} > NO_3 > Fe > F$, whereas during the post-monsoon season it has $Ca^{2+} > Na^+ > K > Mg^{2+}$ and $Cl^- > SO_4 > Fe > HCO_3 > NO_3 > F$. Surface water has $Na^+ > Ca^{2+} > Mg^{2+} > K$ and $Cl^- > HCO_3 > SO_4 > NO_3$, whereas during the post-monsoon phase surface water has $Ca^{2+} > Na^+ > K > Mg^{2+}$ and $Cl^- > SO_4 > Fe > HCO_3 > NO_3 > F$.

4.2.1. pH (Potential of Hydrogen)

pH serves as a crucial physical parameter in water analysis, offering insights into its acidity or alkalinity. It quantifies the concentration of hydrogen ions within the water sample. A pH value of 7 indicates neutrality, with deviations below 7 indicating acidity and values above 7 indicating alkalinity. Indian standards delineate an allowable pH interval from 6.5 to 8.5 without any permissible limit. During the pre-monsoon season, pH levels typically range from 6.6 to 7.9, while during the post-monsoon season, they range from 7.1 to 7.94, as shown in Figure 9.

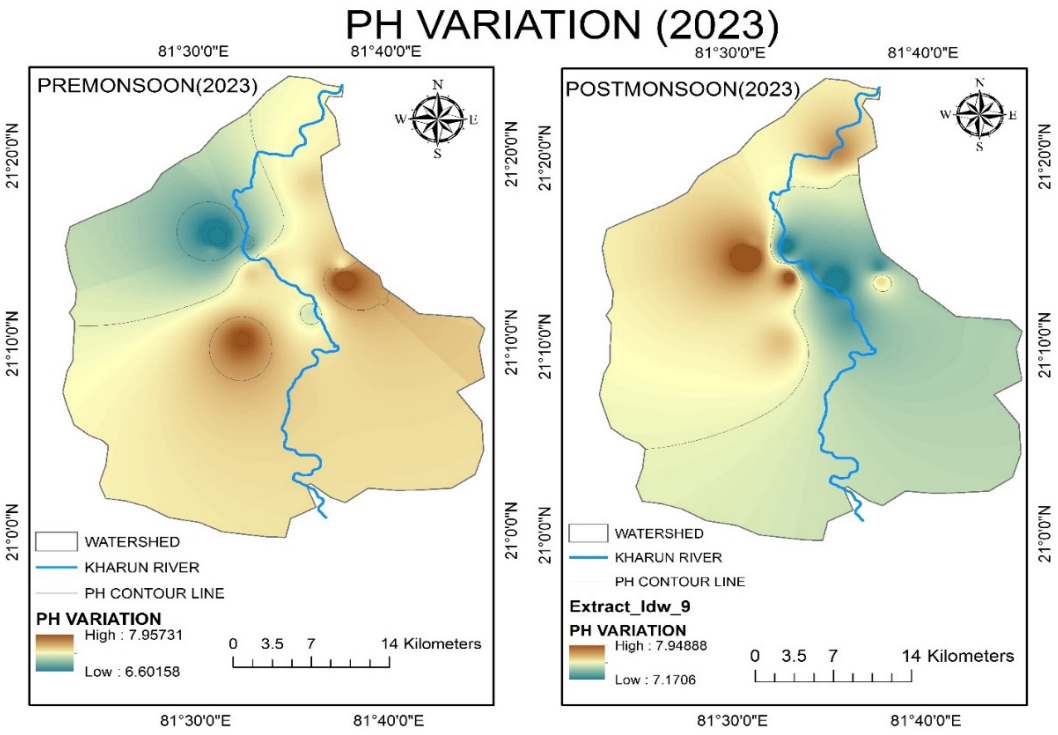


Figure 9. pH variation in groundwater.

4.2.2. Temperature

Temperature is recognized as a significant determinant influencing both chemical and biological phenomena within water bodies. Elevated temperatures correspond to heightened rates of reaction and increased dissolution of chemicals and minerals. In the study region, groundwater samples demonstrated temperatures varying between 27 and 30.8 degrees Celsius in the pre-monsoon period and 21.7 to 25.9 degrees Celsius during the post-monsoon phase, as shown in Figure 10.

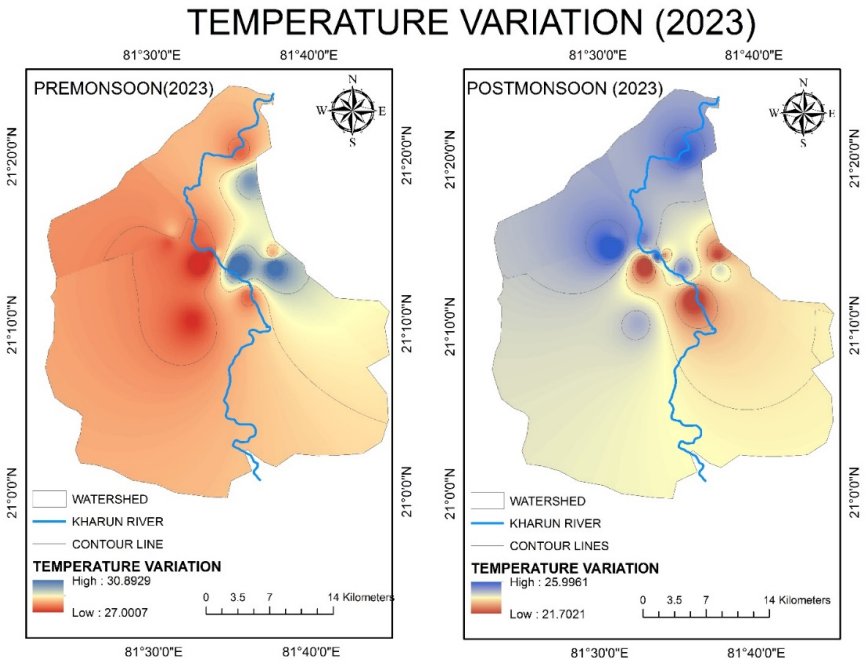


Figure 10. Temperature variation in groundwater.

4.2.3. Total Dissolved Solids (TDS)

The total dissolved solids (TDS) value is calculated as the product of the electrical conductivity (EC) and 0.65. This relationship between TDS and EC is represented by the equation S = EC*K, where EC is measured in micro siemens per centimeter (μS/cm). Here, S denotes the TDS in milligrams per liter, and K signifies the proportionality constant, typically ranging between 0.55 and 0.75. Higher values of K are typically associated with water exhibiting high concentrations of sulfate (Hem, 1985). As per the Bureau of Indian Standards (BIS), the acceptable limit for TDS is 500 mg/L, while the permissible limit is 2000 mg/L. Throughout the pre-monsoon season, TDS levels range from 300.475 to 629.54 mg/L, while during the post-monsoon season they vary between 234.99 and 565.66 mg/L, as shown in Figure 11.

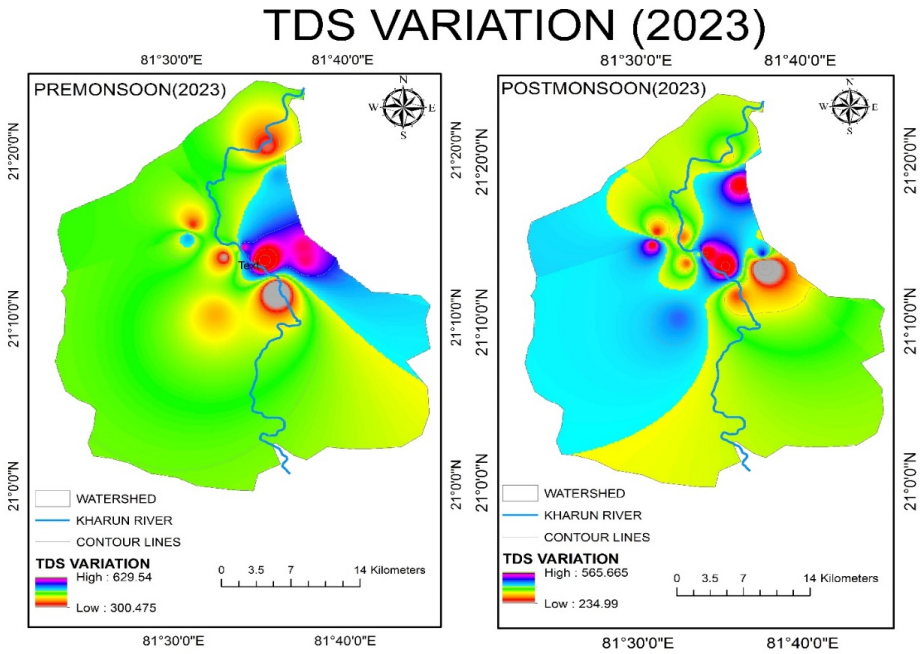


Figure 11. TDS variation in groundwater.

4.2.4. Electrical Conductivity (EC)

Electrical conductivity (EC) serves as a metric for assessing the concentration of dissolved substances within an aqueous solution, reflecting its capacity to conduct electrical current. EC is typically quantified in units known as siemens per unit area (e.g., mS/cm for milli siemens per centimeter or micro siemens per centimeter), as shown in Figure 12. Conventionally, EC measurements are taken at a water temperature of 25 °C. This parameter indicates the abundance of dissolved ionic constituents present in the water, with elevated EC values correlating to higher concentrations of ions.

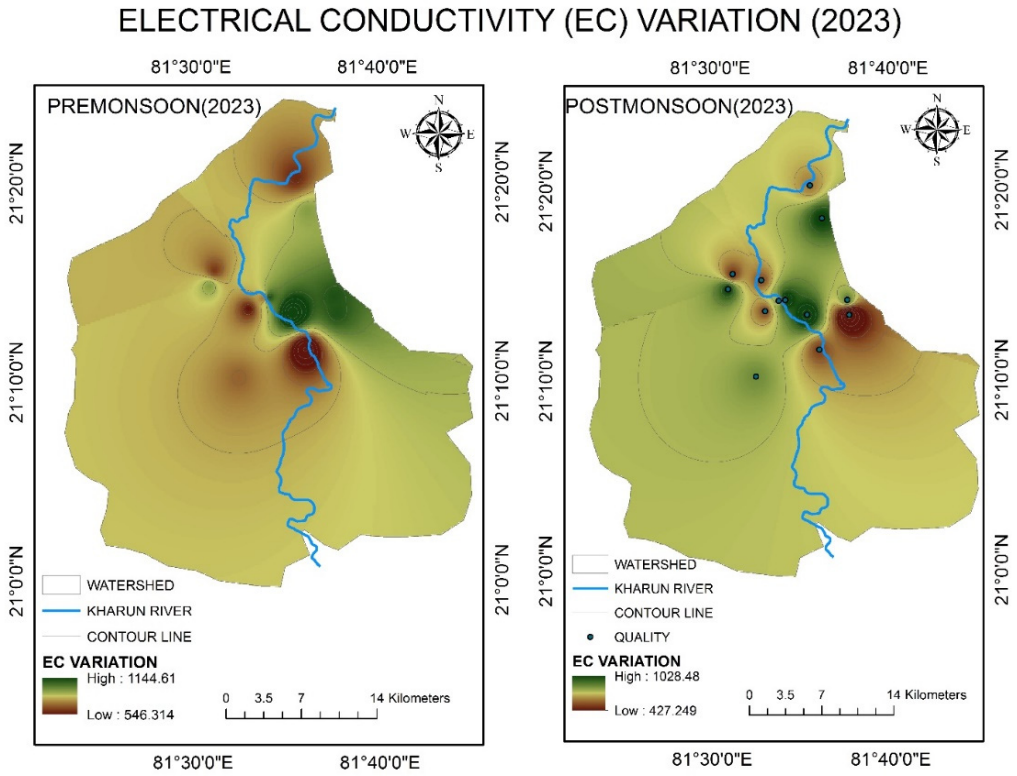


Figure 12. EC variation in groundwater.

4.2.5. Alkalinity

Alkalinity arises from the presence of bicarbonates, carbonates, and hydroxides in water. The weathering of rocks constitutes a primary source of alkalinity, with elevated levels often imparting a bitter taste to water, detrimental to irrigation due to soil damage and the subsequent reduction in crop yields. Carbonate and bicarbonate ions found in groundwater primarily stem from the dissolution of carbon dioxide present in rain and snow, which subsequently dissolves additional carbon dioxide upon infiltration into the soil. The solubility of carbon dioxide diminishes with an increase in temperature and a decrease in pressure, while organic matter decay releases additional carbon dioxide for dissolution. As per the BIS and WHO, the pH of water delineates the form of carbon dioxide present, with pH levels below 4.5 indicating carbonic acid, pH levels between 4.5 and 8.3 suggesting the presence of bicarbonates, and pH levels exceeding 8.2 indicating the presence of carbonates. Under typical conditions, bicarbonate concentrations in groundwater may range from 100 to 800 ppm, contributing to water alkalinity and hardness.

Bicarbonate content serves as a key indicator of total alkalinity within the region. In the research area, the alkalinity of groundwater spans from 1.5 to 9.4 mg/L as $CaCO_3$ in the pre-monsoon period and from 6.6 to 33.32 mg/l during the post-monsoon period, as shown in Figure 13.

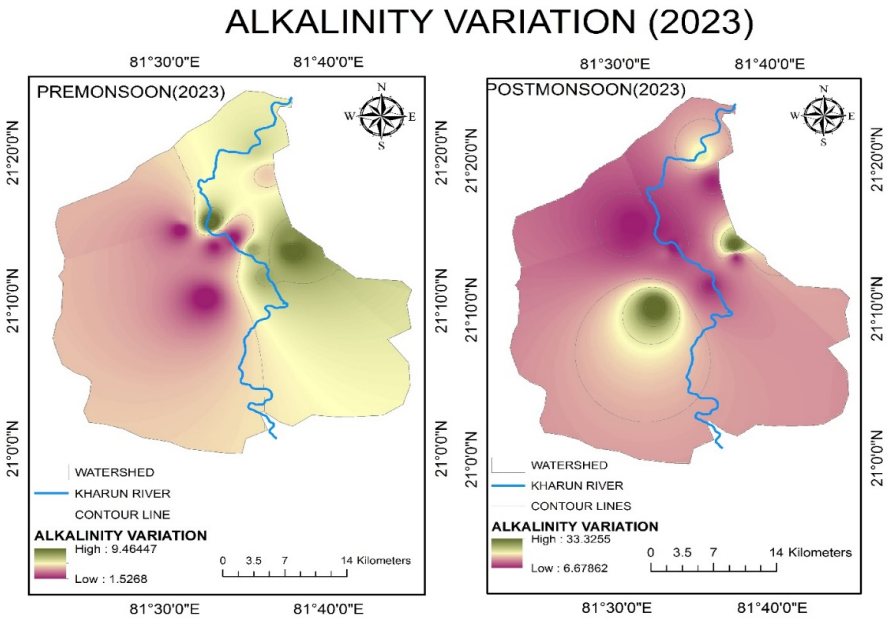


Figure 13. Alkalinity variation in groundwater.

4.2.6. Chloride (Cl^-)

Chloride represents a significant constituent in groundwater, despite its minimal presence in crustal rocks. Several mechanisms contribute to heightened chloride concentrations in groundwater, encompassing evaporation, recurrent evaporation coupled with salt dissolution, interactions with evaporitic formations, water entrapment during sedimentation, and the influx of seawater. Chloride salts exhibit high solubility and typically remain in the form of sodium chloride without undergoing chemical reactions with minerals from the reservoir rock. Pollution from chloride-rich effluents originating from sewage and municipal waste may also contribute to heightened chloride concentrations in water sources. The documented chloride concentrations span from 11.66 to 26.96 mg/L in the pre-monsoon period and from 36.82 to 173.615 mg/L in the post-monsoon period, all of which remain within the maximum allowable thresholds established by the Bureau of Indian Standards (BIS) at 1000 mg/L, as shown in Figure 14.

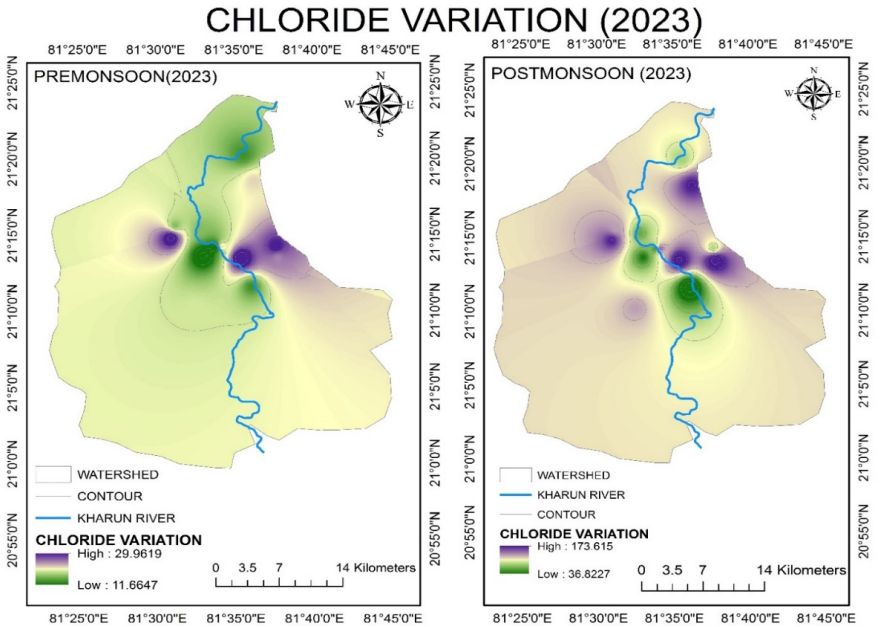


Figure 14. Chloride variation in groundwater.

4.2.7. Total Hardness (TH)

Water characterized by high levels of hardness is not recommended for drinking purposes due to its propensity to deposit scale on water heaters, pipelines, and kitchenware and its elevated consumption of soap during laundering. The total hardness levels in groundwater samples obtained from the study area vary from 235.03 to 559.566 mg/L as $CaCO_3$ during the pre-monsoon season and from 182.053 to 554.864 mg/L during the post-monsoon season, as shown in Figure 15.

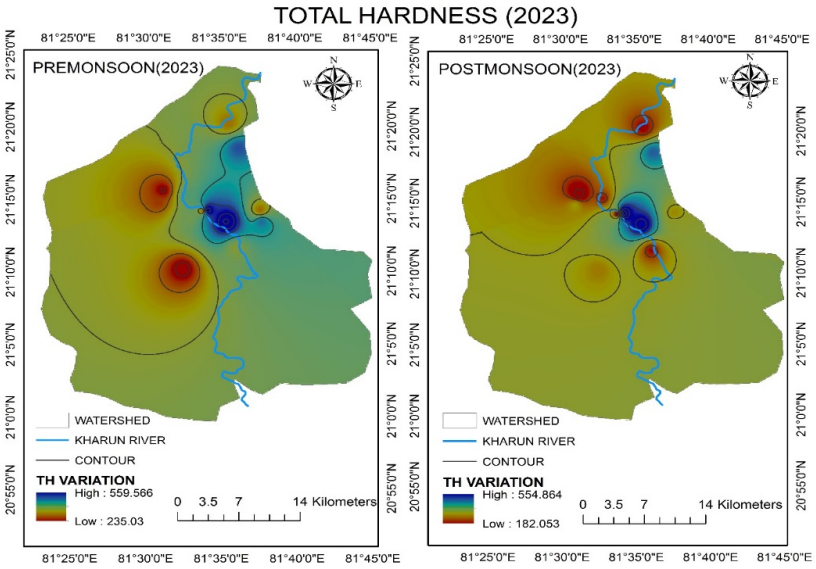


Figure 15. Total hardness variation in groundwater.

4.2.8. Calcium (Ca^{2+})

Calcium, as the fifth most prevalent naturally occurring element, permeates freshwater systems primarily through the erosion of various rock formations, notably limestone, although other minerals such as marble, calcite, dolomite, gypsum, fluorite, and apatite also play contributory roles. Additionally, it infiltrates from the soil via seepage, leaching, and runoff processes. In the study area, groundwater calcium concentrations fluctuate between 58.73 and 156.02 mg/L during the pre-monsoon season and from 19.22 mg/L to 138.63 mg/L during the post-monsoon season, as shown in Figure 16.

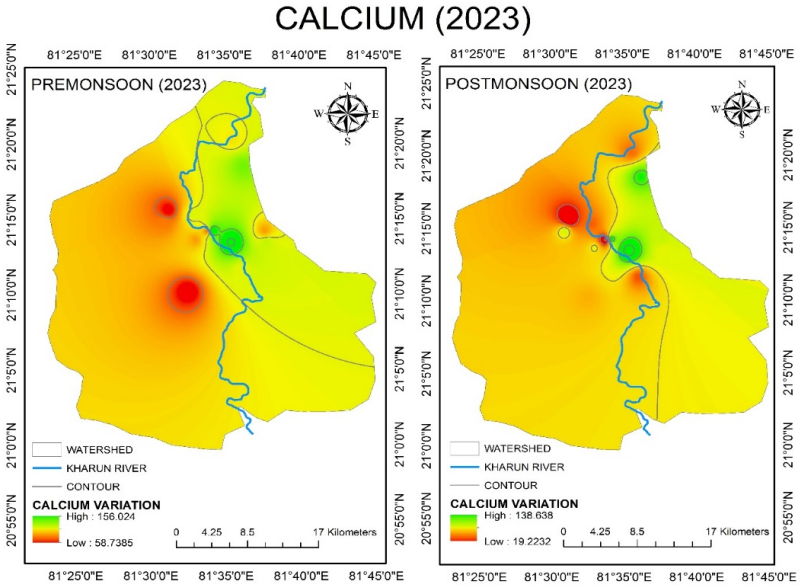


Figure 16. Calcium variation in groundwater.

4.2.9. Magnesium (Mg^{2+})

Magnesium (Mg) ranks as the eighth most abundant natural element. Its presence in drinking water can impart undesirable tastes, with some individuals perceiving unpleasant flavours at concentrations as low as 100 mg/L, while the average person may find the taste disagreeable at approximately 500 mg/L. Furthermore, elevated magnesium levels in drinking water, particularly exceeding 700 mg/L as magnesium sulfate, may induce a laxative effect. In groundwater samples collected during the pre-monsoon season, magnesium concentrations range from 17.25 to 41.53 mg/L, while during the post-monsoon season they vary from 18.71 to 66.34 mg/L, as shown in Figure 17.

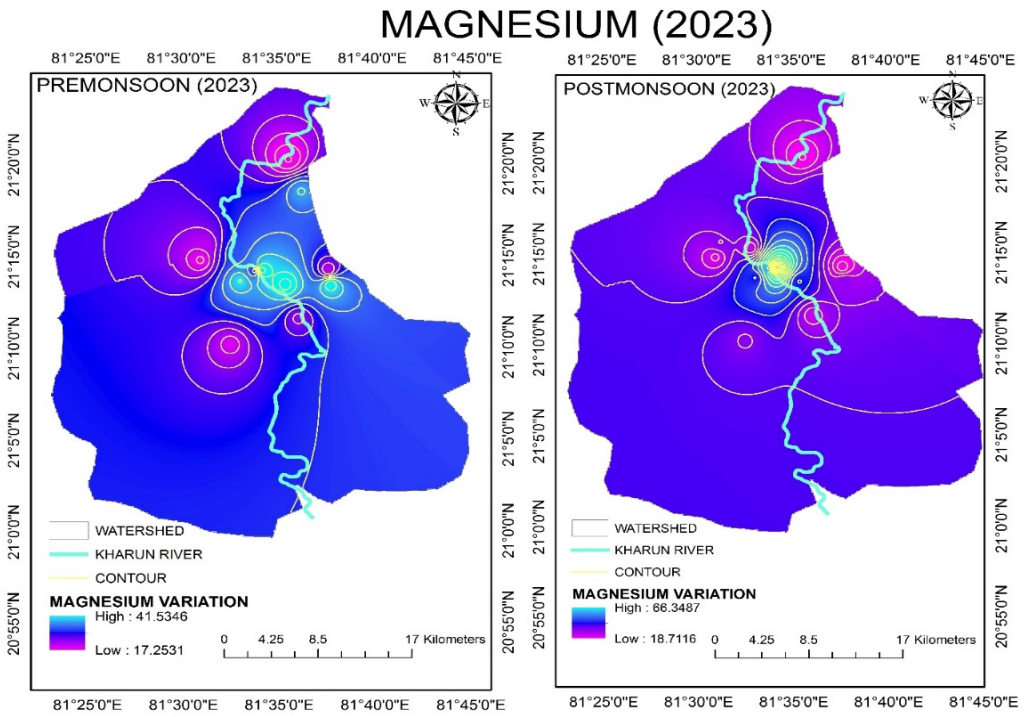


Figure 17. Magnesium variation in groundwater.

4.2.10. Sodium (Na^{+})

Sodium, ranking sixth among the most abundant elements globally, exhibits wide distribution across various environmental compartments including soils, vegetation, aquatic systems, and dietary sources. Abundant reservoirs of sodium-rich minerals, notably sodium chloride or common salt, are present in numerous geographical regions worldwide. Naturally occurring in groundwater, sodium manifests no discernible odor but imparts a detectable taste when its concentration exceeds 200 milligrams per liter (mg/L) for most individuals. Owing to the prevalence of sodium compounds within geological formations and soil matrices, groundwater universally contains certain levels of sodium due to the dissolution of these compounds in water. In the study area, the range of Na+ ions in groundwater samples varies from 10.232 to 39.97 mg/L during the pre-monsoon season and from 14.972 to 64.447 mg/L during the post-monsoon season, as shown in Figure 18.

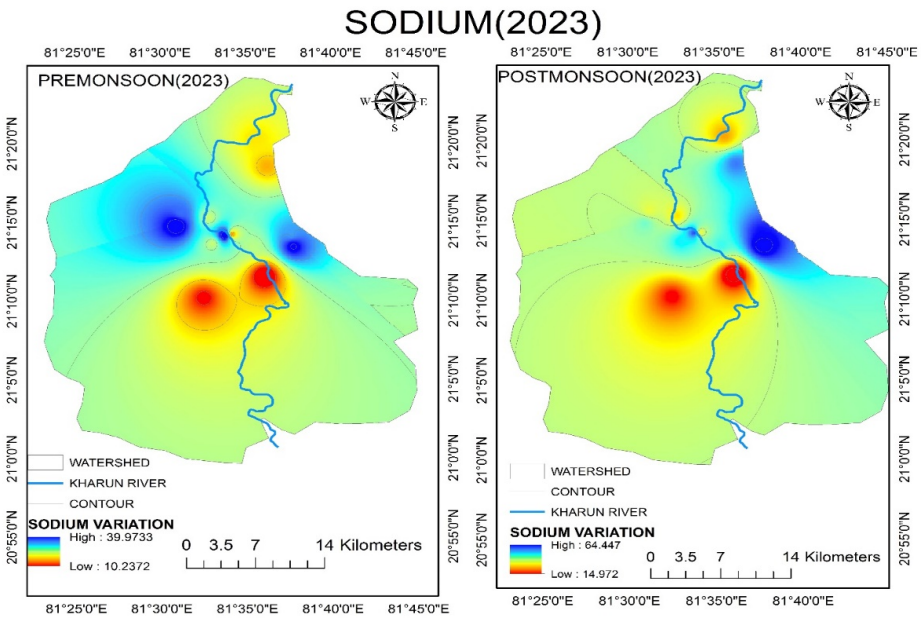


Figure 18. Sodium variation in groundwater.

4.2.11. Potassium (K^+)

Potassium, an element occurring naturally, is frequently encountered in geological formations like soils and rocks. Its presence in water typically does not introduce any noticeable odor or color, although it may contribute to a faintly salty flavor. As a positively charged ion, potassium has the propensity to be adsorbed by negatively charged colloidal constituents existing in soil and rock matrices, including silicate clay minerals, iron and aluminum oxides, as well as organic colloids. The degree of potassium adsorption is contingent upon the nature and quantity of colloids available. For instance, peat, characterized by an abundance of highly charged organic colloids, is capable of adsorbing significantly more potassium compared with sandy soils, which contain fewer colloids. In water samples collected during the pre-monsoon season, the concentration of K^+ ions ranges from 4.3 to 222.9 mg/L, while during the post-monsoon season it varies from 0.83 to 73.4 mg/L, as shown in Figure 19.

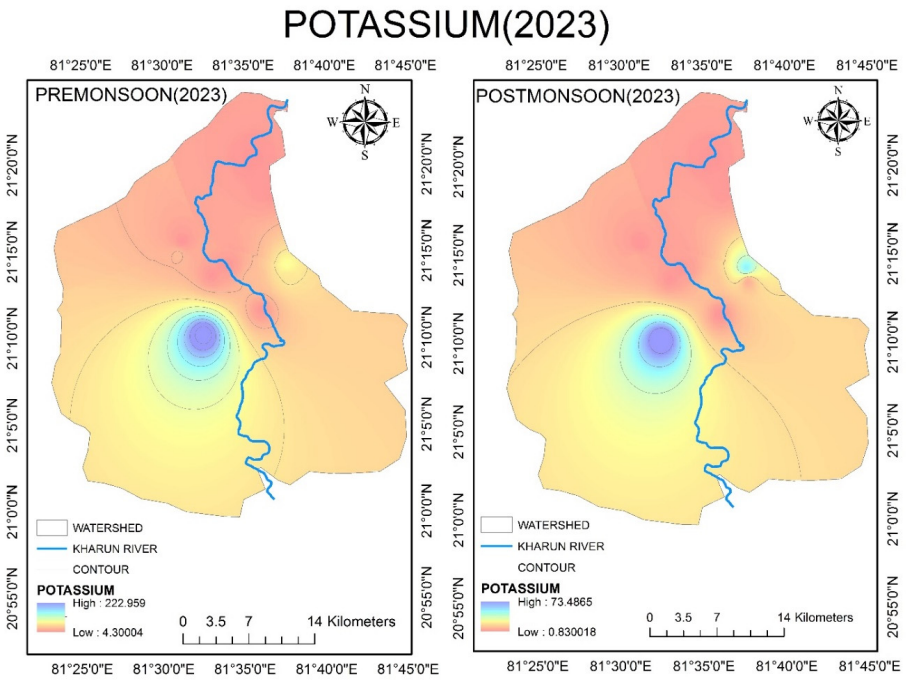


Figure 19. Potassium variation in groundwater.

4.3. Groundwater and Surface Water Interaction Study

4.3.1. Rock–Water Interaction Study

Piper Trilinear Diagram

The study employed a Piper trilinear diagram (Figure 20) to analyze water samples, aiming to understand groundwater dynamics (Piper, 1944; Xia et al., 2018). Most samples fell into Zones I and II, indicating calcium–magnesium–chloride–sulfate and sodium–potassium–chloride–sulfate groundwater types. Over 50% of pre-monsoon and over 85% of post-monsoon samples were in Zone 1, showing a predominance of alkaline earth ions. Almost all samples were in Zone 4, suggesting strong acid dominance. Less than 50% of pre-monsoon and about 15% of post-monsoon samples were in Zone 2, indicating that alkalis surpassed alkaline earth ions. Zone 3 had no samples, indicating weak acid dominance. Additionally, Zone 6 contained 50% or more of both pre-monsoon and post-monsoon samples, representing chloride–calcium groundwater. The majority fell into Zone A (calcium type) and Zone B (no dominant type). Zone G (chloride type) encompassed all pre-monsoon and over 90% of post-monsoon samples.

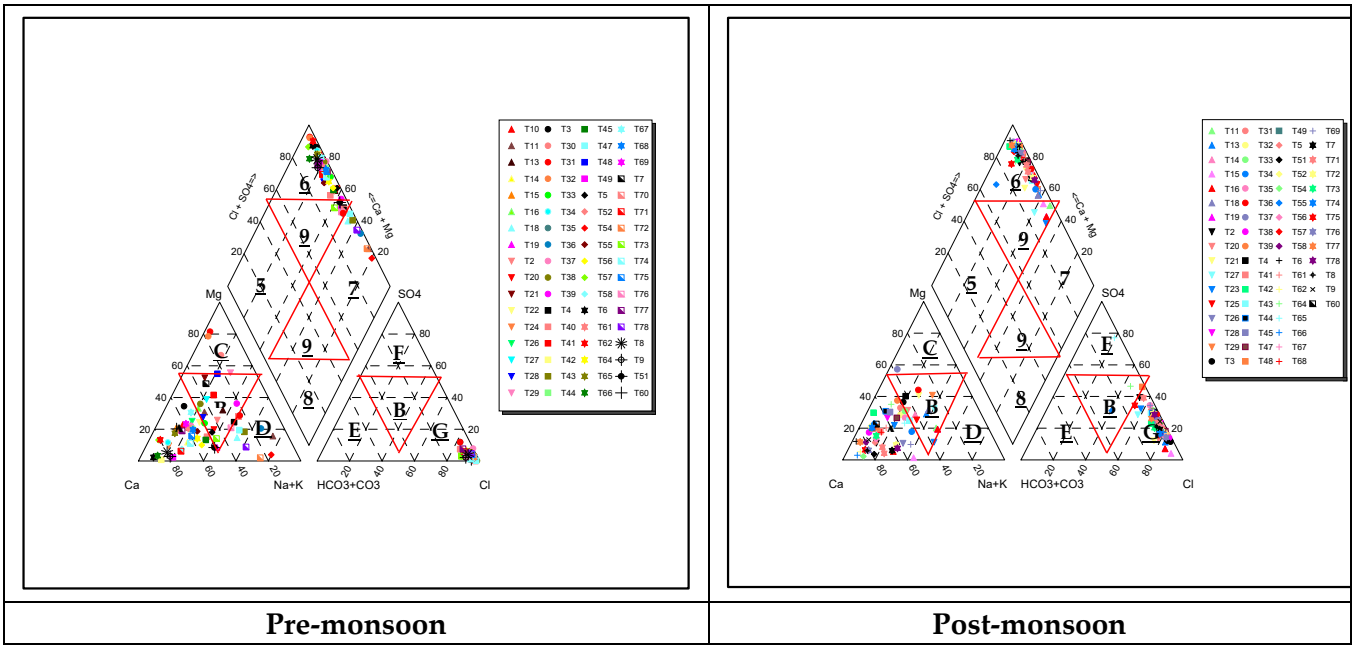


Figure 20. Piper diagram of groundwater.

This study employed Piper diagrams (Figure 21) to analyze the chemical composition of the Kharun River's surface water, correlating it with groundwater hydrochemistry. About 80% of pre-monsoon and all post-monsoon samples fell within Zone I and Zone II, indicating calcium–magnesium–chloride–sulfate dominance over sodium–potassium–chloride–sulfate. No samples fell into Zone III or Zone IV, indicating the absence of sodium–potassium–bicarbonate and calcium–magnesium–bicarbonate water. Over 80% of pre-monsoon samples and all post-monsoon samples were in Zone 1, showing a predominance of alkaline earth ions. Almost all samples fell into Zone 4, with no samples in Zone 3, indicating strong acid dominance. More than 60% of pre-monsoon and all post-monsoon samples were in Zone 6, representing chloride–calcium-type water. Approximately 15% of pre-monsoon samples fell into Zone 7, indicating chloride–sodium-type water. None fell into Zone 5 or Zone 8. Around 20% of pre-monsoon samples and 40% of post-monsoon samples were in Zone A, while approximately 60% of samples were in Zone B. A total of 20% of pre-monsoon samples were in Zone D, with no samples in Zone C. None fell

into Zone E or Zone F during the pre-monsoon period, but 30% of post-monsoon samples were in Zone F, representing sulfate-type water. All pre-monsoon samples and over 50% of post-monsoon samples were in Zone G, representing chloride-type water.

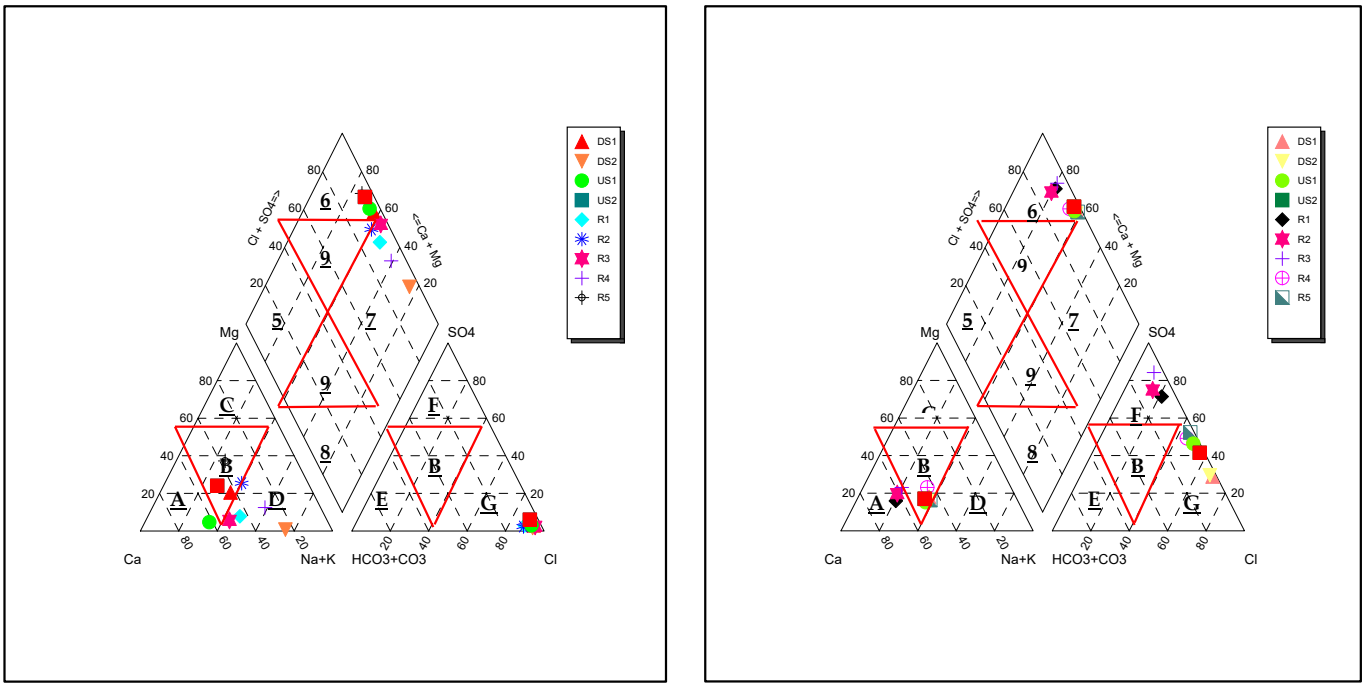


Figure 21. Piper diagram of surface water.

Gibbs Diagram

The chemical composition of groundwater is a key determinant of its suitability for domestic and agricultural use. This composition is primarily governed by three major factors: the rate of evaporation, atmospheric precipitation patterns, and interactions between water and geological formations. To better understand these influences, Gibbs developed the Gibbs diagram, which categorizes groundwater chemistry based on dominant controlling mechanisms. As shown in Figure 22, most sampled water points fall within the rock dominance field, indicating that chemical weathering of rock minerals is a major factor influencing groundwater quality. However, several data points lie outside the defined dominance fields. This deviation suggests potential mixing between rainwater and rock-influenced groundwater or other hydrogeochemical processes, such as anthropogenic inputs or localized variations in recharge sources. Further investigation into these anomalies is necessary to better understand their implications for groundwater quality and its sustainable management.

In this study, Gibbs diagrams were applied to surface water, depicted in Figure 23, to comprehend groundwater's influence on it. The presented Gibbs diagrams reveal that a notable portion of river water samples conform to the rock dominance classification, indicating a potential mineral mixing process. This finding implies that rock minerals sourced from groundwater may contribute to the composition of surface water.

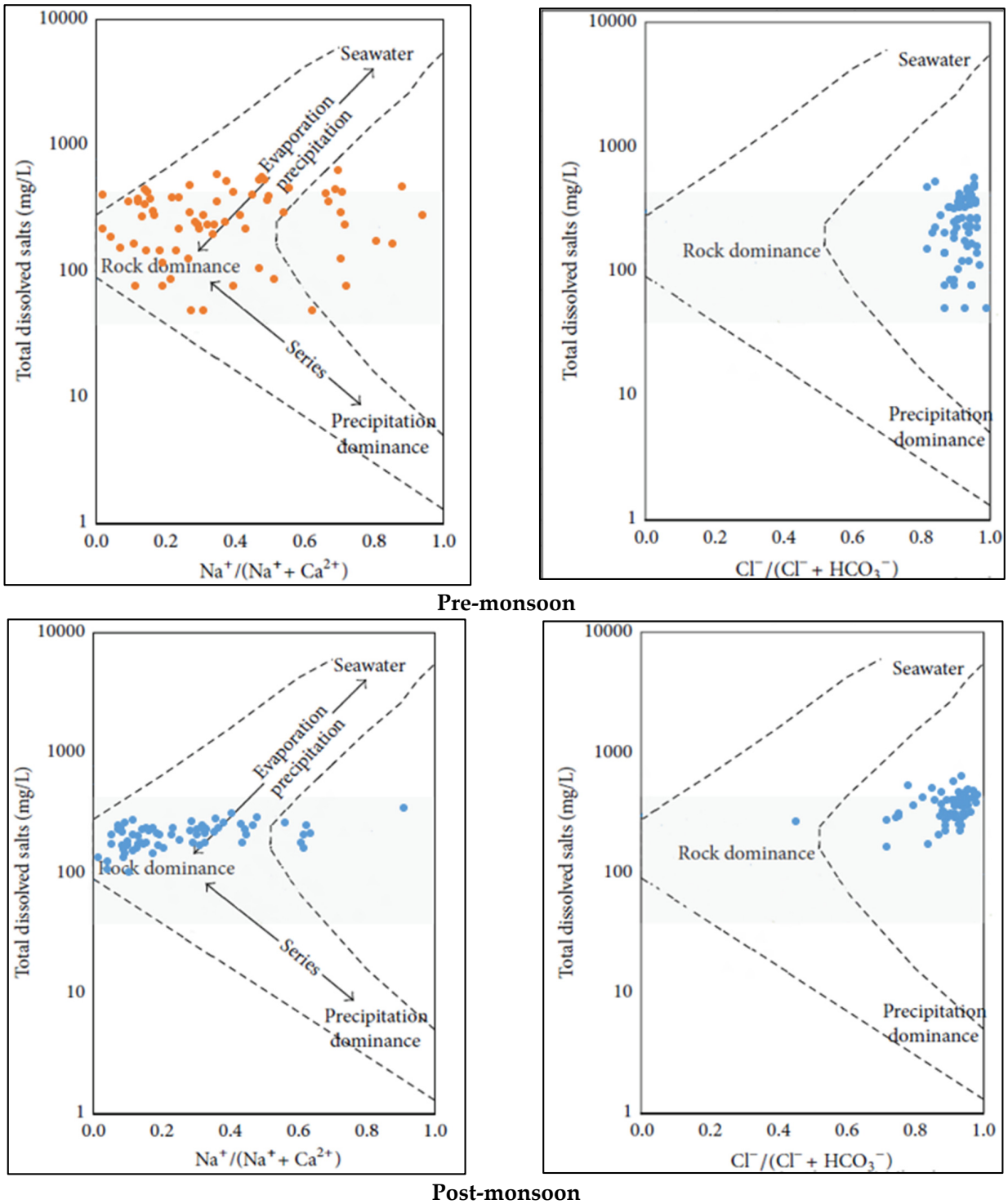


Figure 22. Gibbs diagram of groundwater.

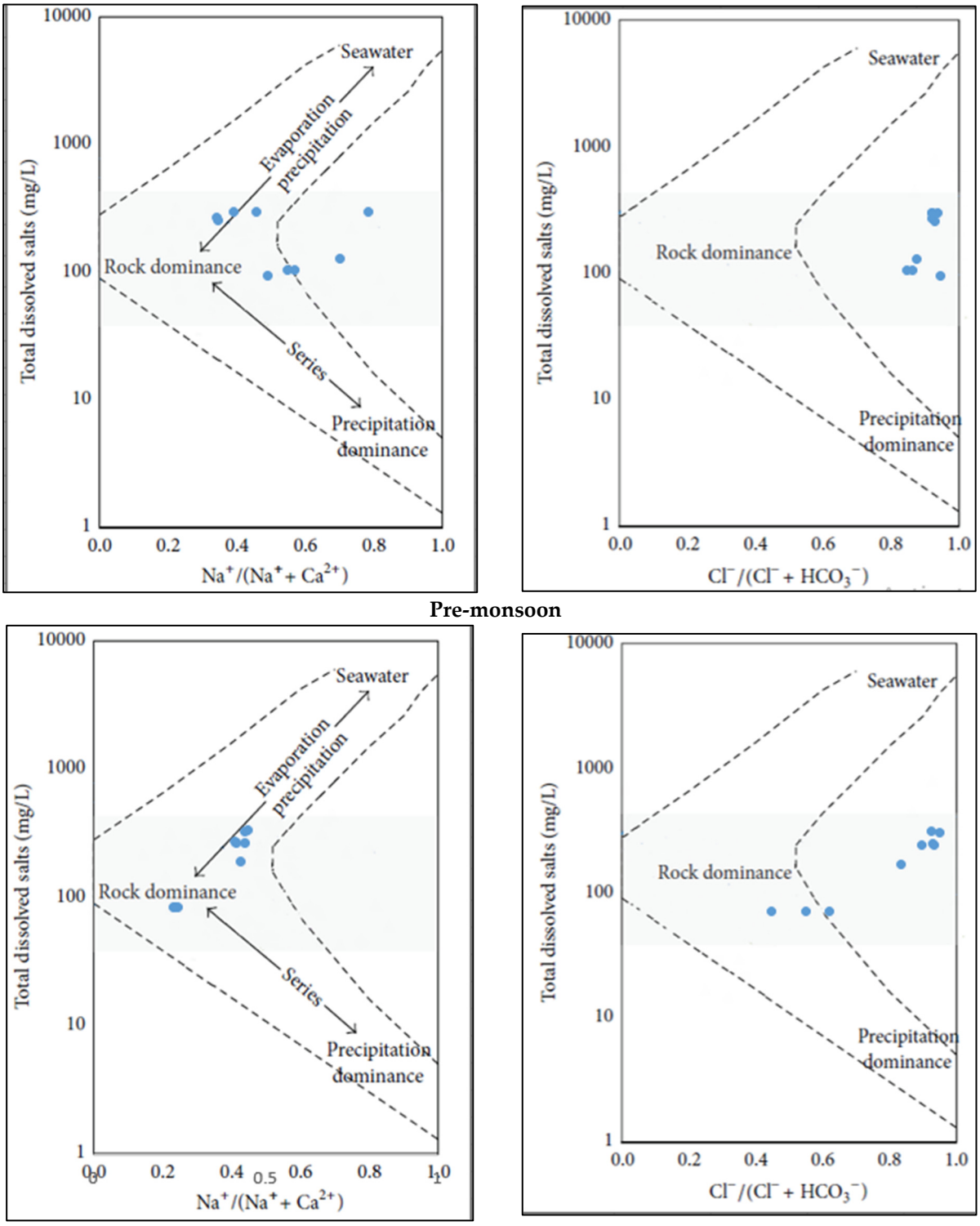


Figure 23. Gibbs diagram of surface water.

4.3.2. Statistical Study

Pearson Correlation Analysis

Correlation analysis is a widely applied statistical method in water quality assessment used to identify the key factors influencing water chemistry [44]. It unveils the associations between variables [45]. A positive correlation signifies a simultaneous increase in monitored parameters, while a negative correlation indicates an inverse relationship [46]. The

correlation coefficient (R) ranges from +1 to −1, where a strong correlation lies between ±0.8 and ±1.0, a moderate correlation between ±0.5 and ±0.8, and a weak correlation from 0.0 to ±0.5 [46,47].

Tables 1–4 present Pearson correlation matrices for borehole and surface water samples during the pre-monsoon and post-monsoon seasons. The analysis reveals distinct hydrogeochemical processes influencing groundwater and surface water chemistry.

During the pre-monsoon phase, a strong correlation exists between TDS and EC (r^2 = 1.00). A moderate correlation exists between EC and Mg (r^2 = 0.53), EC and Ca (r^2 = 0.51), EC and Cl (r^2 = 0.61), TDS and Mg (r^2 = 0.53), TDS and Ca (r^2 = 0.51), and TDS and Cl (r^2 = 0.61). Considerable human activities are responsible for introducing these ions into the local groundwater. Furthermore, this elucidates the presence of anthropogenic sources, such as deteriorated sewer pipelines.

Table 1. Pearson correlation matrix for groundwater during the pre-monsoon season in 2022 (Sampling Site: 70).

	pH	Temp	Cond(EC)	TDS	Na	K	Mg	Ca	Fe	F	Cl	SO_4	HCO_3	NO_3
pH	1.00													
Temp	0.22	1.00												
Cond	−0.41	0.08	1.00											
TDS	−0.41	0.08	**1.00**	1.00										
Na	−0.12	−0.20	0.40	0.40	1.00									
K	−0.23	−0.14	0.17	0.17	0.20	1.00								
Mg	−0.09	0.02	**0.53**	**0.53**	0.12	0.05	1.00							
Ca	−0.57	−0.21	**0.51**	**0.51**	0.18	0.14	−0.08	1.00						
Fe	−0.19	−0.08	0.12	0.12	0.22	0.14	−0.07	0.12	1.00					
F	0.26	0.13	0.17	0.17	0.22	−0.03	0.14	−0.21	0.25	1.00				
Cl	−0.21	0.09	**0.61**	**0.61**	0.27	−0.04	0.35	0.31	0.11	0.06	1.00			
SO_4	0.04	−0.14	−0.09	−0.09	−0.17	0.04	−0.04	−0.14	−0.12	0.07	−0.10	1.00		
HCO_3	−0.38	−0.17	0.25	0.25	−0.01	0.05	0.08	0.36	0.13	−0.06	0.21	−0.04	1.00	
NO_3	−0.39	−0.39	0.29	0.29	0.22	−0.04	0.14	0.43	0.05	−0.17	0.25	−0.08	0.29	1.00

Table 2. Pearson correlation matrix for groundwater during the post-monsoon season in 2022 (Sampling Site: 70).

	pH	Temp	Cond(EC)	TDS	Na	K	Mg	Ca	Fe	F	Cl	SO_4	HCO_3	NO_3
pH	1.00													
Temp	0.13	1.00												
Cond	−0.04	−0.26	1.00											
TDS	−0.04	−0.26	**1.00**	1.00										
Na	0.10	−0.30	**0.53**	**0.53**	1.00									
K	−0.18	−0.34	0.36	0.36	0.12	1.00								
Mg	−0.26	0.06	0.14	0.14	0.14	0.29	1.00							
Ca	−0.39	−0.12	0.14	0.14	−0.06	−0.02	−0.24	1.00						
Fe	0.16	0.03	−0.04	−0.04	−0.04	0.09	−0.12	0.08	1.00					
F	0.13	0.02	0.20	0.20	0.27	0.23	0.10	0.01	0.07	1.00				
Cl	−0.27	−0.10	**0.61**	**0.61**	0.18	0.08	0.18	0.37	−0.11	0.05	1.00			
SO_4	−0.20	−0.11	0.43	0.43	0.11	0.24	0.16	0.07	−0.07	0.22	0.44	1.00		
HCO_3	−0.01	−0.41	0.47	0.47	0.32	0.32	0.07	−0.16	−0.16	0.13	−0.01	0.06	1.00	
NO_3	0.00	−0.02	0.07	0.07	0.05	−0.08	−0.25	0.17	−0.10	−0.30	0.09	−0.12	0.03	1.00

Table 3. Pearson correlation matrix for surface water during the pre-monsoon period in 2022 (Sampling Site: 09).

	pH	Temp	Cond	TDS	Na	K	Mg	Ca	Cl	SO_4	HCO_3	NO_3
pH	1.00											
Temp	0.45	1.00										
Cond	−0.87	−0.42	1.00									
TDS	−0.87	−0.42	**1.00**	1.00								
Na	−0.20	0.45	0.26	0.26	1.00							
K	−0.86	−0.37	**0.95**	**0.95**	0.24	1.00						
Mg	−0.29	−0.50	0.30	0.30	−0.48	0.11	1.00					
Ca	−0.52	−0.08	**0.66**	**0.66**	**0.59**	**0.77**	−0.47	1.00				
Cl	−0.69	−0.41	**0.65**	**0.65**	0.23	**0.61**	−0.04	**0.59**	1.00			
SO_4	−0.75	−0.77	**0.53**	**0.53**	−0.40	**0.53**	**0.54**	0.04	0.46	1.00		
HCO_3	−0.19	−0.20	0.17	0.17	0.35	0.08	0.08	0.18	0.16	−0.11	1.00	
NO_3	0.27	0.04	−0.68	−0.68	−0.26	−0.63	−0.01	−0.63	−0.45	0.09	0.02	1.00

Table 4. Pearson correlation matrix for surface water during the post-monsoon season in 2022 (Sampling Site: 09).

	pH	Temp	Cond	TDS	Na	K	Mg	Ca	Cl	SO_4	HCO_3	NO_3
pH	1.00											
Temp	0.46	1.00										
Cond	−0.88	−0.45	1.00									
TDS	−0.88	−0.45	**1.00**	1.00								
Na	−0.86	−0.43	**1.00**	**1.00**	1.00							
K	−0.90	−0.42	**0.98**	**0.98**	**0.98**	1.00						
Mg	−0.73	−0.25	**0.94**	**0.94**	**0.95**	**0.90**	1.00					
Ca	−0.89	−0.53	**0.98**	**0.98**	**0.98**	**0.96**	**0.91**	1.00				
Cl	−0.91	−0.49	**0.97**	**0.97**	**0.97**	**0.97**	**0.90**	**0.98**	1.00			
SO_4	−0.67	−0.25	0.54	0.54	0.53	0.69	0.39	0.51	0.63	1.00		
HCO_3	−0.64	−0.13	0.54	0.54	0.51	0.50	0.42	0.51	0.53	0.42	1.00	
NO_3	−0.79	−0.51	**0.81**	**0.81**	**0.79**	**0.83**	0.72	**0.83**	**0.88**	0.62	0.30	1.00

Similar to the pre-monsoon phase, a strong correlation exists between TDS and EC (r^2 = 1.00), while the moderate correlations between EC and Na, EC and Cl, TDS and Na, and TDS and Cl (r^2 = 0.53–0.61) suggest ion-exchange and mineral-weathering processes. The slight shifts in correlation patterns between seasons may be attributed to increased recharge and dilution effects during the post-monsoon period.

A strong correlation in surface water during the pre-monsoon period between EC and TDS (r^2 = 1.00) and major ions such as K, Ca, and Cl suggests that silicate weathering is a key process. Moderate correlations between EC and Ca, Cl, and SO_4 (r^2 = 0.53–0.66) further support mineral dissolution from rock formations. The presence of significant ion associations, such as K-SO_4 and Mg-SO_4, indicates contributions from both natural weathering and possible agricultural runoff.

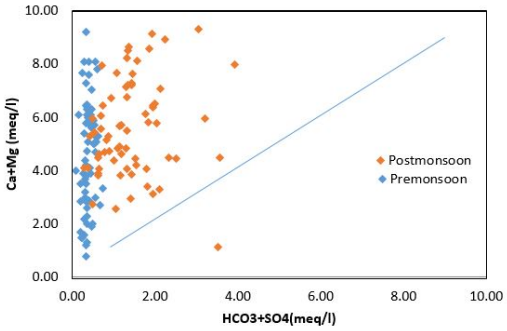
In the post-monsoon phase, strong correlations among multiple parameters, including EC and TDS, EC and Na, EC and K, and EC and Ca (r^2 = 0.94–1.00), highlight the dominance of silicate weathering. High correlations between Na and Ca (r^2 = 0.98), Na and

Cl (r^2 = 0.97), and K and Cl (r^2 = 0.97) suggest ion-exchange and dolomitization processes, likely driven by the dissolution of Cl-rich minerals such as amphiboles and biotite. Increased water–rock interactions following monsoon recharge may enhance these processes.

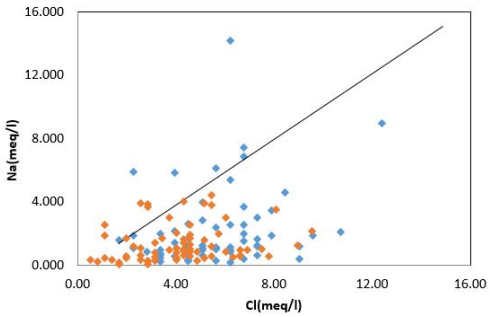
The key processes influencing water chemistry in the study area include silicate weathering, ion exchange and dolomitization, anthropogenic influences, and seasonal recharge effects. Silicate weathering plays a significant role, as evidenced by strong correlations among Na, K, Ca, and Mg with EC and TDS, indicating that rock weathering substantially impacts water composition. Ion exchange and dolomitization are also evident, with associations such as Na–Ca, Na–Mg, and Mg–Ca suggesting active cation exchange and carbonate dissolution processes. Additionally, the anthropogenic influence is reflected in the presence of Cl and SO_4 correlations, which point to potential contamination from human activities, including sewage infiltration and agricultural runoff. Lastly, seasonal recharge effects alter correlation patterns, particularly post-monsoon, when dilution from increased groundwater recharge enhances interactions with geological formations. Understanding these processes is essential for effective water resource management and pollution control.

Scatter Plots

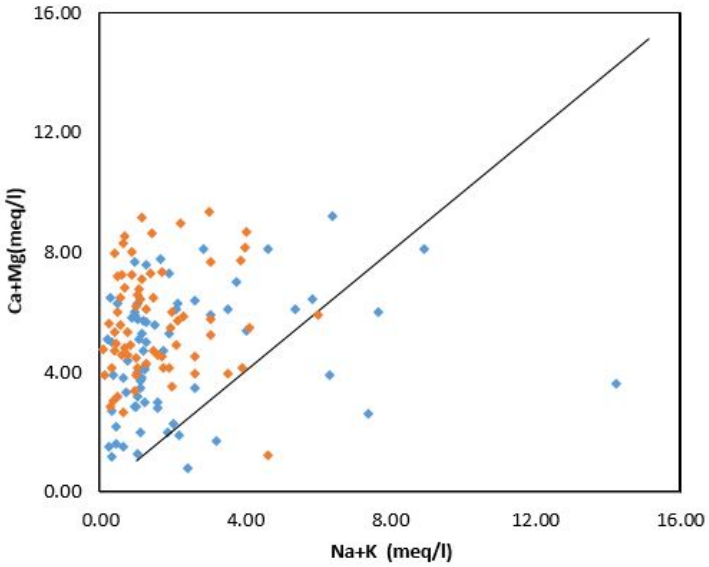
The scatter plots in Figure 24 (groundwater) and Figure 25 (surface water) provide a comparative analysis of major ion relationships, highlighting the distinct hydrogeochemical processes governing each water type. While both datasets examine similar ionic interactions, the differences between groundwater and surface water chemistry are evident in their scatter patterns and distribution trends.



$(Ca^{2+} + Mg^{2+})$ vs. $(SO_4^{2-} + HCO_3^-)$



Na^+ vs. Cl^-



$(Ca^{2+} + Mg^{2+})$ vs. $(Na^+ + K^+)$

Figure 24. Scatter plots of groundwater.

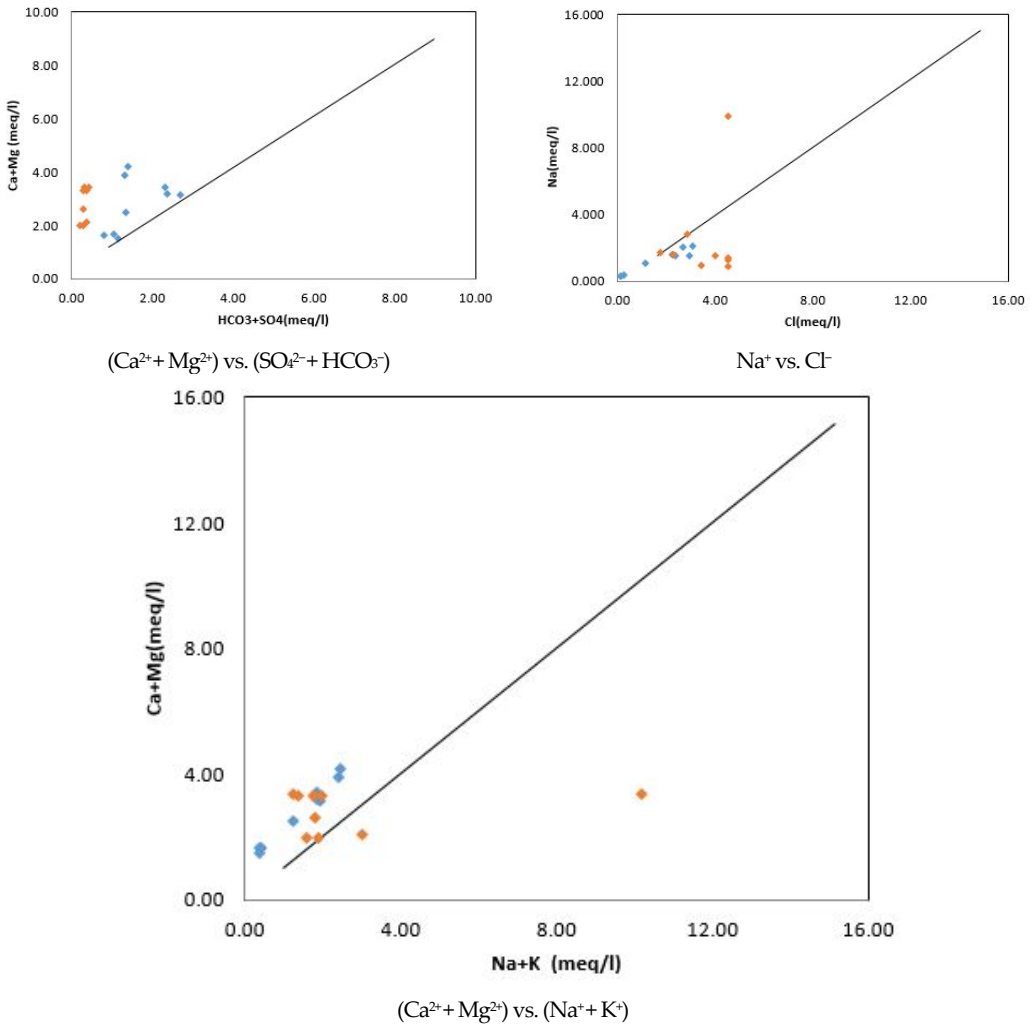


Figure 25. Scatter plots of surface water.

In the (Ca^{2+} + Mg^{2+}) vs. ($SO_4{}^{2-}$ + $HCO_3{}^{-}$) plot, groundwater samples (Figure 24) generally lie above the equiline, indicating an excess of alkaline earth metals due to carbonate weathering and gypsum dissolution. Post-monsoon samples show greater dispersion, suggesting increased dissolution and recharge effects. In contrast, surface water samples (Figure 25) cluster more closely along the equiline, implying a near balance between Ca^{2+} + Mg^{2+} and $SO_4{}^{2-}$ + $HCO_3{}^{-}$, which suggests a more direct influence of atmospheric deposition and surface runoff rather than prolonged rock–water interactions.

The Na^+ vs. Cl^- plot further illustrates these differences. In groundwater, most data points fall below the equiline, indicating an excess of chloride over sodium. This imbalance suggests that factors such as anthropogenic influences (agriculture, industrial contamination) and cation exchange processes affect groundwater chemistry. Meanwhile, surface water samples display a more aligned trend along the equiline, indicating halite dissolution or evaporative effects as the primary controls on Na–Cl concentrations, with less impact from ion exchange reactions.

The (Ca^{2+} + Mg^{2+}) vs. (Na^+ + K^+) plot highlights the distinct evolutionary pathways of groundwater and surface water. Groundwater samples exhibit greater deviation from the equiline, reinforcing the role of cation exchange and silicate weathering in altering the ionic balance. This trend, particularly prominent in post-monsoon samples, reflects the prolonged interaction of groundwater with minerals. Conversely, surface water samples remain more closely clustered along the equiline, suggesting that its chemical composition is

primarily governed by direct weathering inputs and atmospheric influences, with minimal ion exchange effects.

Overall, the groundwater chemistry exhibits greater variability and a larger seasonal influence, with trends suggesting prolonged rock–water interaction, ion exchange, and anthropogenic contributions. In contrast, surface water maintains a more direct chemical signature of precipitation and runoff, with less evidence of long-term geochemical alteration. These differences highlight how groundwater undergoes continuous mineral dissolution and ion exchange, while surface water reflects short-term hydrological interactions with more stable ionic relationships.

Hierarchical Cluster Analysis (HCA)

Cluster analysis is a powerful statistical technique used to classify objects based on shared characteristics, making it a valuable tool for interpreting hydrochemical processes in water quality studies. In this research, hierarchical clustering was applied to identify patterns in groundwater and surface water chemistry. The Euclidean distance metric was used to measure similarity among water quality variables, while Ward's method was employed as the clustering criterion to minimize variance within clusters. The use of cluster analysis for categorizing objects based on similarities has been well documented [48–50].

To enhance accuracy, data normalization was performed using min–max normalization before analysis, and clustering was conducted using PAST 4.03 software (Paleontological Statistics (https://www.nhm.uio.no/english/research/resources/past/, accessed on 20 July 2023)). This approach allowed for a systematic categorization of monitoring stations based on their hydrochemical attributes. The results, visualized through dendrograms (Figures 26 and 27), reveal the formation of four distinct groundwater clusters (C1, C2, C3, and C4). Additionally, surface water samples formed a separate cluster, positioned between clusters C1 and C2, indicating a transitional hydrochemical nature influenced by both groundwater and surface water interactions.

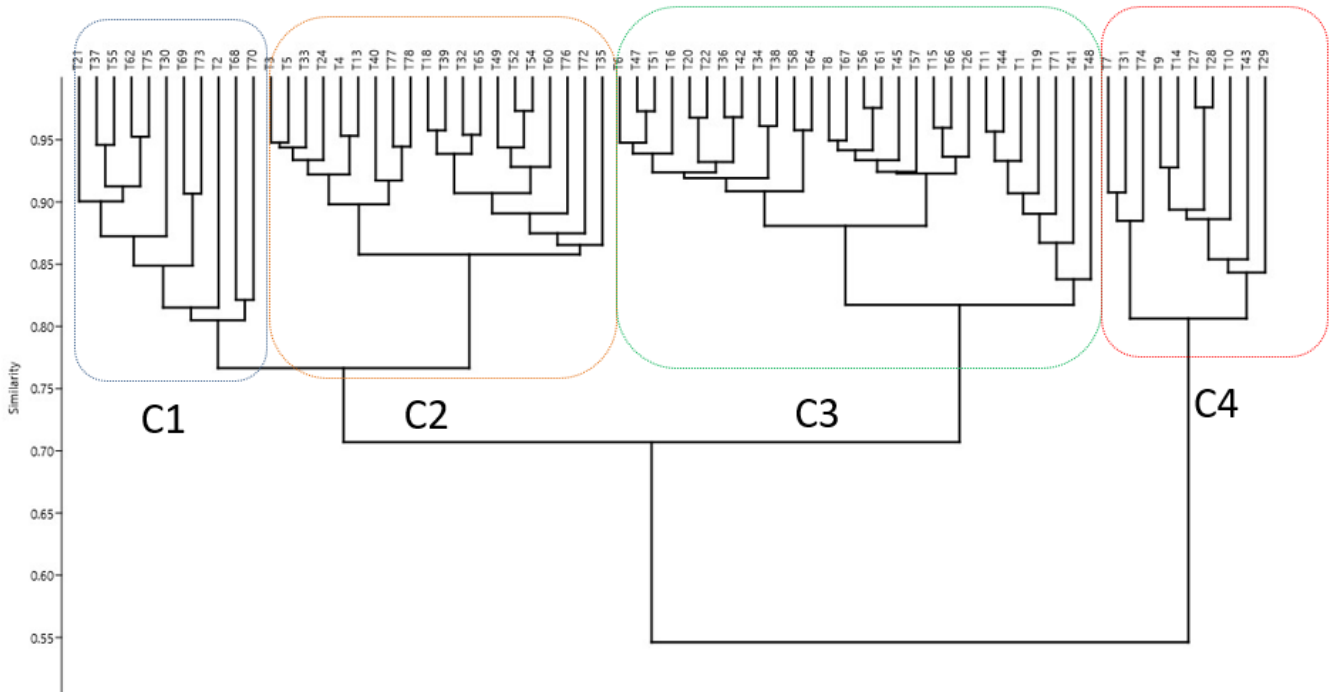


Figure 26. Hierarchical cluster analysis in groundwater.

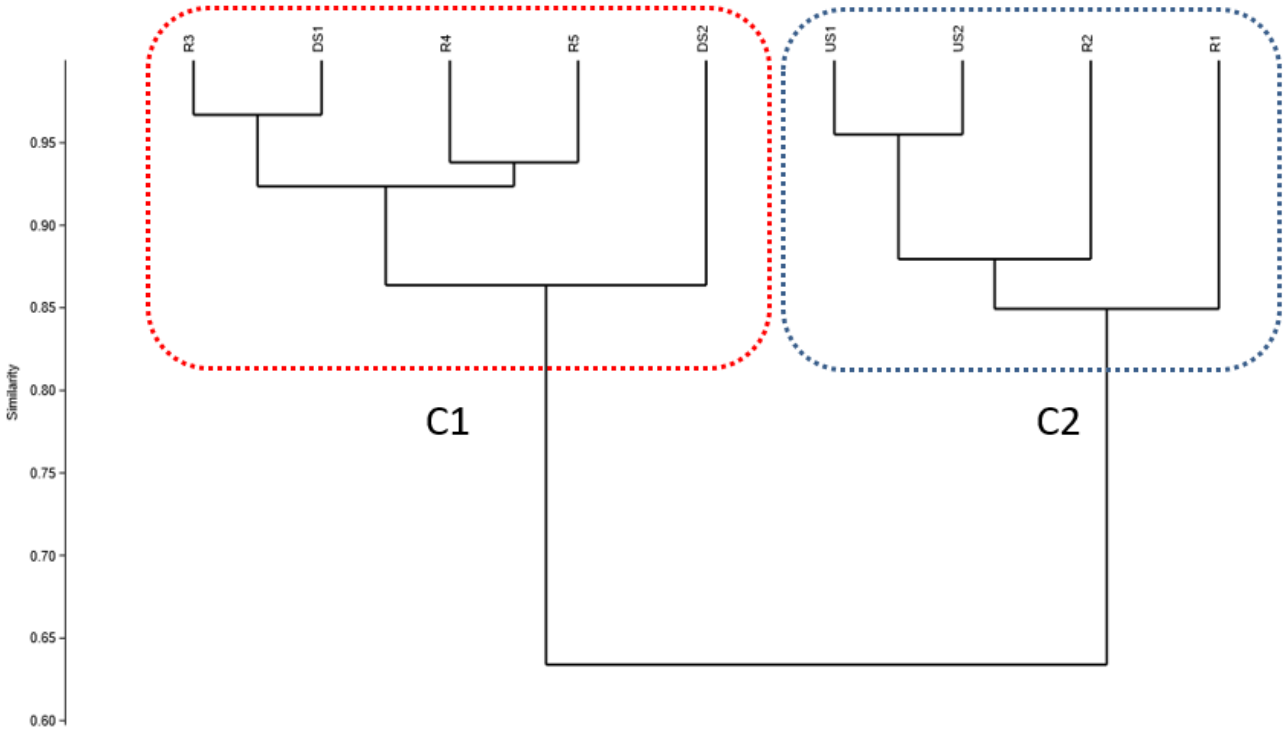


Figure 27. Hierarchical cluster analysis in surface water.

The clustering results provide critical insights into the dominant hydrochemical processes shaping water quality across the study area. The distinct grouping patterns suggest variations in mineral dissolution, ion exchange, and anthropogenic influences across different locations. Moreover, the positioning of the surface water cluster relative to groundwater clusters highlights potential recharge interactions or pollution influences. These findings underscore the importance of cluster analysis in distinguishing hydrochemical regimes and guiding sustainable water management strategies.

4.3.3. Stable Isotope Study

a) Local Meteoric Water Line (LMWL) Development

Groundwater, being an integral component of the water cycle, assimilates traces from various interacting sources, thus undergoing changes in both its quality and quantity. Effective resource management mandates a comprehensive understanding of potential groundwater sources in a given region, necessitating consideration of secondary sources to ascertain the actual water budget. Although evaluating groundwater ionic concentrations and comparing them with surface water compositions can offer insights into recharge sources, variations stemming from localized pollutants and solid wastes may confound interpretations. Accordingly, employing stable isotopes of water emerges as the most reliable and efficient approach for source identification. As isotopic content remains unaffected by environmental factors and water quality degradation, hydrogen and oxygen isotopes serve as robust indicators for this purpose. Isotopic variations primarily stem from processes such as evaporation, latitudinal and altitudinal variances, and water mixing, particularly in regions characterized by diverse topography and land cover. In such areas, understanding the interplay between various water bodies and groundwater is crucial. The current study area, despite its plain topography and lack of significant latitudinal or altitudinal variations, hosts numerous ponds that could impact groundwater recharge, particularly during the summer season. Consequently, efforts are directed toward elucidating the similarity

between groundwater and surface water to discern the precise contributions of each source to groundwater recharge.

The findings are presented in relation to the Vienna Standard Mean Ocean Water and are articulated using conventional notation (δ‰, Equation (1)), with a precision of δD 1‰ and $\delta^{18}O$ 0.1‰.

$$\delta‰ = \left[\frac{R_{Sample}}{R_{Standard}} - 1\right] \times 1000 \quad (1)$$

Samples obtained during both the pre-monsoon and post-monsoon periods underwent analysis for oxygen and hydrogen isotopes to investigate the varied influences of distinct sources on groundwater.

b) $\delta^{18}O$ and $\delta^{2}H$ Isotopic Composition of Precipitation

To evaluate the hydrogen and oxygen isotopic composition of precipitation in the Raipur region, four samples were collected during the post-monsoon period. The $\delta^{18}O$ values ranged from −13.05‰ to −7.40‰, with an average of −10.43‰, while $\delta^{2}H$ values varied between −90.91‰ and −51.51‰, with a mean of −73.52‰ as shown in Table 5. These values were plotted on the Global Meteoric Water Line (GMWL) to examine their alignment with global precipitation patterns and to derive the Local Meteoric Water Line (LMWL) for the study area.

Table 5. Stable isotope data of groundwater and surface water samples.

Type of Water	$\delta^{18}O$		$\delta^{2}H$		D-Excess	
	Min	**Max**	**Min**	**Max**	**Min**	**Max**
Borewell	−7.35	−1.52	−32.884	−16.42	−4.26	36.54
Dugwell	−4.6	−1.66	−34.47	−8.244	−12.75	25.99
Pond	2.19	5.85	−4.266	12.712	−34.087	−21.786
River	−3.53	−2.66	−32.21	−25.83	−8.21	−3.459
Precipitation	−13.055	−7.40	−90.91	−51.50	6.431	13.524

The LMWL equation, determined using linear regression, was:

$$\delta^{2}H = 6.8149\ \delta^{18}O - 2.4403\ (r^2 = 1.00)$$

In comparison, the GMWL equation follows the standard relation:

$$\delta^{2}H = 8\ \delta^{18}O + 10\ (r^2 = 1.00)$$

The slope of the LMWL (6.81) is lower than that of the GMWL (8.00), suggesting secondary evaporation effects that influence the isotopic composition of precipitation before infiltration, as shown in Figure 28. However, the derivation of the LMWL from only four precipitation samples introduces potential limitations, as a more robust LMWL typically requires a larger dataset encompassing seasonal variations. Additionally, given the relatively flat topography of the study area, altitude-related fractionation effects were considered negligible.

To enhance the reliability of the LMWL, future studies should incorporate a greater number of precipitation samples across multiple seasons, allowing for a more comprehensive assessment of isotopic variability in the region.

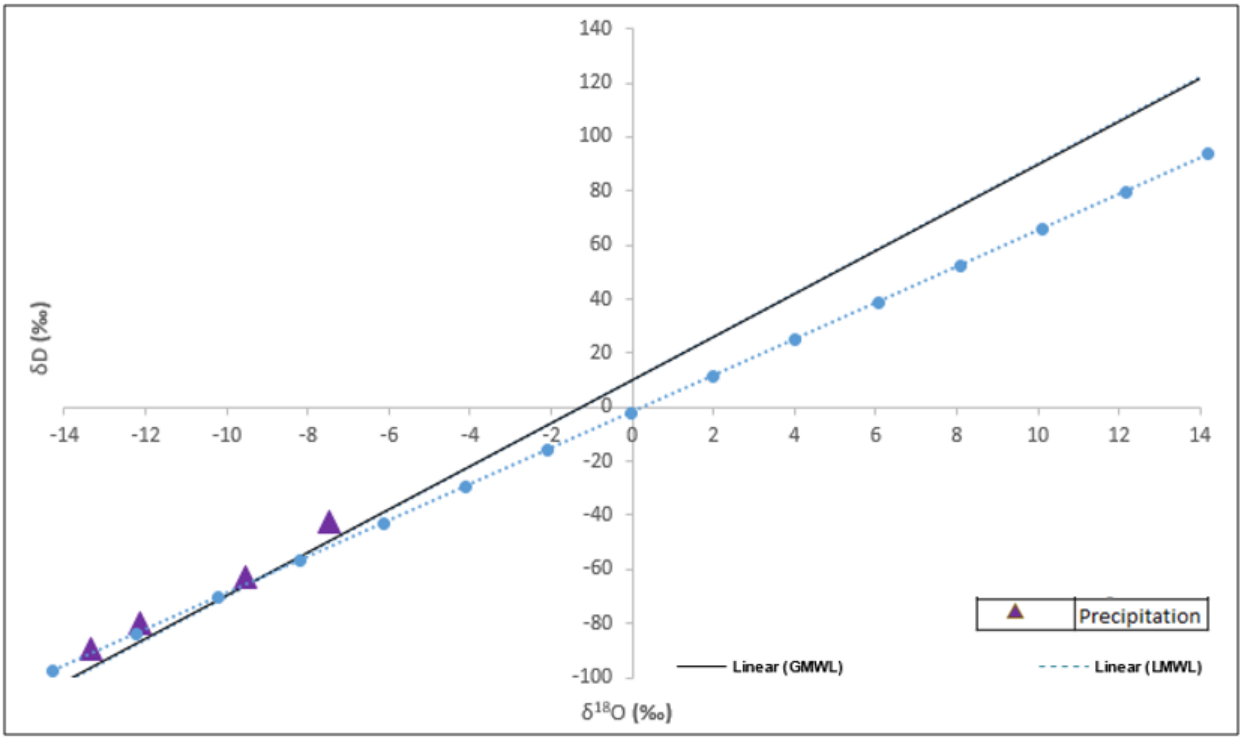


Figure 28. Linear plot of $\delta^{18}O$ and $\delta^{2}H$ for precipitation samples.

c) $\delta^{18}O$ and $\delta^{2}H$ Isotopic Composition of Surface Water and Groundwater

The oxygen and hydrogen isotopic composition of surface water and groundwater in the study area exhibits notable variability. Pond water shows $\delta^{18}O$ values ranging from 2.19‰ to 5.85‰, with corresponding $\delta^{2}H$ values between −4.27‰ and 12.71‰, while river water displays $\delta^{18}O$ values from −3.53‰ to −2.66‰ and $\delta^{2}H$ values from −32.21‰ to −25.83‰. In groundwater, $\delta^{18}O$ values range from −7.35‰ to −1.52‰ for bore wells and −4.6‰ to −1.66‰ for dug wells, while $\delta^{2}H$ values vary from −32.88‰ to −16.42‰ in bore wells and −34.47‰ to −8.24‰ in dug wells.

The $\delta^{18}O$ vs. $\delta^{2}H$ plot highlights significant evaporative enrichment in river and pond samples, as indicated by their deviation from the Local Meteoric Water Line (LMWL). The Kharun River LMWL equation ($\delta^{2}H = 6.6228\ \delta^{18}O - 9.1679$) and the Pond LMWL equation ($\delta^{2}H = 5.0434\ \delta^{18}O - 14.582$) both exhibit slopes lower than the Global Meteoric Water Line (GMWL), confirming the influence of evaporation. Groundwater samples, particularly from dug wells and bore wells, predominantly align with the LMWL, suggesting minimal evaporative effects. However, two outliers (one bore well and one dug well) deviate from this trend, indicating potential influences such as localized evaporation, mixing with surface water, or anthropogenic inputs, as shown in Figure 29.

The clear resemblance between certain groundwater and surface water samples suggests hydraulic connectivity between these sources. Specifically, dug wells—being more vulnerable to atmospheric interactions—demonstrate isotopic signatures closer to surface water, reinforcing the likelihood of shallow aquifer recharge from river or pond water. The observed outliers (marked by red dots and black diamonds) could be attributed to site-specific conditions, including differential recharge rates, localized evaporation effects, or mixing with isotopically enriched sources. Further investigation, such as seasonal sampling and hydrochemical analysis, would help clarify the exact mechanisms influencing these variations. Furthermore, the resemblance observed between groundwater and surface water samples signifies an interaction between the two water sources.

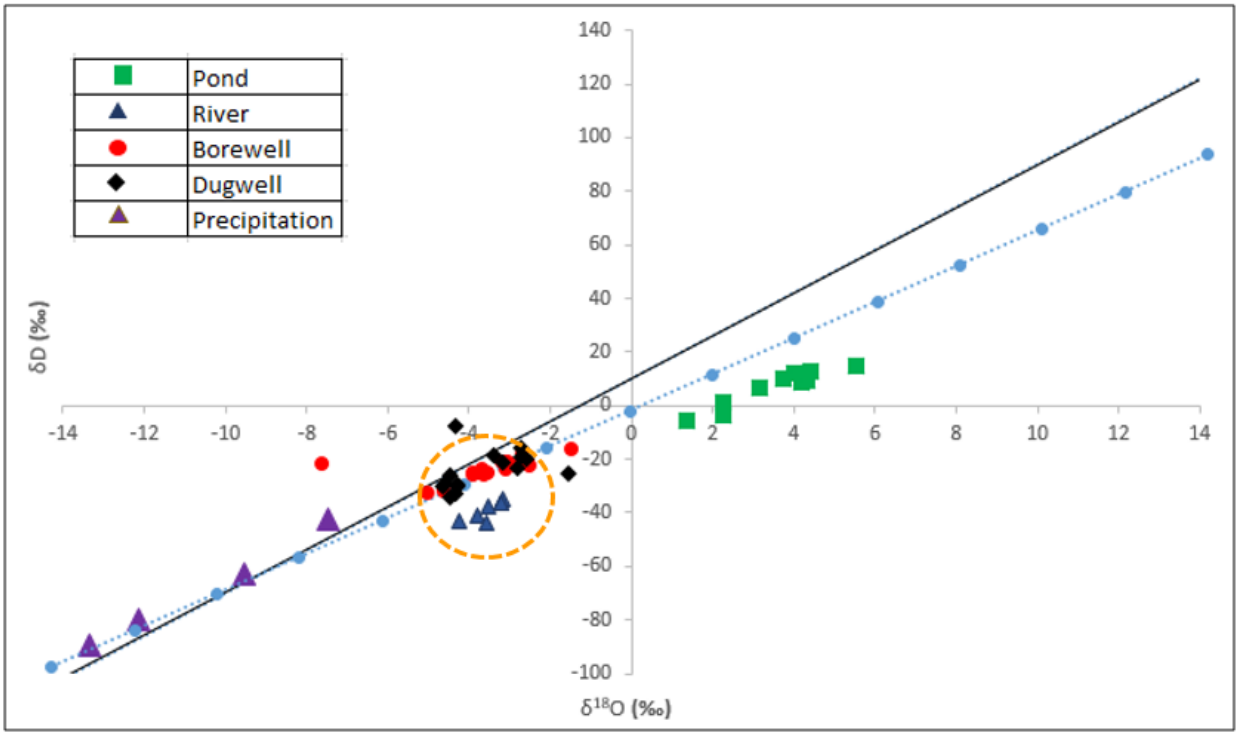


Figure 29. Plot representing δ^2H vs. $\delta^{18}O$ for water samples.

d) Deuterium Excess of the Samples

Deuterium excess (D-excess) serves as a key tracer for identifying non-equilibrium fractionation processes in the hydrological cycle, reflecting the combined influences of evaporation, relative humidity, ocean surface temperature, wind speed, and the origin of atmospheric moisture. Reductions in D-excess typically indicate enhanced evaporative effects, leading to isotopic enrichment in the residual water phase and an increase in the vapor phase.

The calculated D-excess values for precipitation in the study area range from 6.43‰ to 13.52‰, aligning with Global Meteoric Water Line (GMWL) trends and indicating minimal deviation from equilibrium conditions. In contrast, surface water bodies, such as ponds and the Kharun River, exhibit significantly lower D-excess values, ranging from −34.09‰ to −21.79‰ and −8.21‰ to −3.46‰, respectively. This marked depletion suggests substantial evaporative enrichment, particularly in stagnant water bodies like ponds. Groundwater samples, including bore wells and dug wells, show a broader D-excess range (−4.26‰ to 36.54‰ for bore wells and −12.75‰ to 25.99‰ for dug wells), reflecting site-specific variations in recharge processes, aquifer interactions, and localized evaporation effects.

Analysis of the $\delta^{18}O$ vs. D-excess plot (Figure 30) highlights distinct clustering patterns, suggesting variable degrees of evaporative influence across different water sources. While surface water samples (ponds and rivers) demonstrate significant evaporation-induced isotopic enrichment, most groundwater samples align closely with the Local Meteoric Water Line (LMWL), indicating a dominant meteoric recharge component with minimal evaporative modification. However, the presence of a few outlier groundwater samples, particularly those deviating toward lower D-excess values, suggests possible mixing with evaporated surface water or a prolonged residence time in the unsaturated zone.

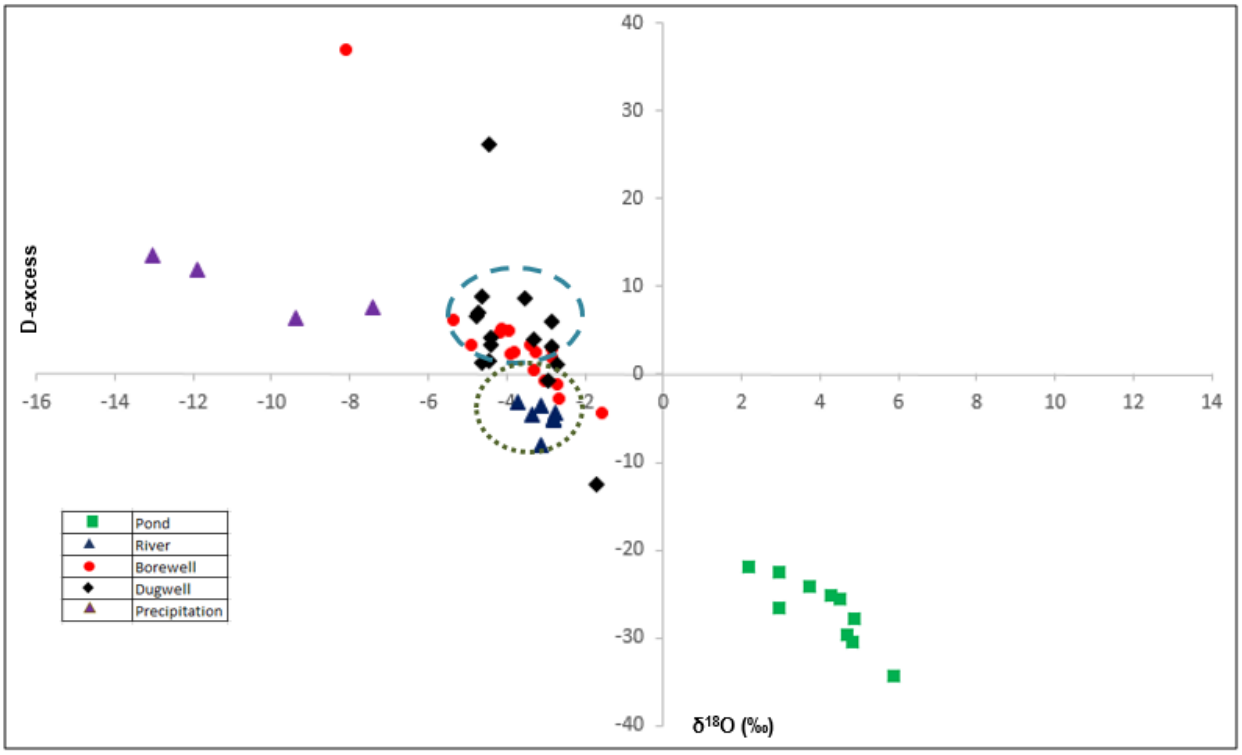


Figure 30. Plot representing D-excess vs. δ18O.

The urbanized nature of the Raipur region, characterized by planned settlements, vegetation cover, and controlled water use, appears to mitigate significant groundwater evaporation. In contrast, agricultural zones undergoing seasonal fallow periods during summer experience increased evapotranspiration, contributing to localized isotopic enrichment. This highlights the need for seasonal monitoring to further quantify evaporation-driven isotopic shifts and their implications for groundwater sustainability.

5. Conclusions

This study highlights the intricate hydrological dynamics governing surface water and groundwater interactions in Raipur, India, a region experiencing rapid urbanization and escalating water demand. The hydrochemical and isotopic analyses reveal significant anthropogenic influences on water quality, with clear evidence of contamination from agricultural runoff, industrial discharge, and urban effluents. Correlation and cluster analyses indicate distinct geochemical signatures, pointing to silicate weathering as a dominant natural process, alongside notable contributions from anthropogenic sources such as sewage infiltration and fertilizer application.

Stable isotope analysis provides compelling evidence of groundwater–surface water exchange, particularly in river-adjacent bore wells and dug wells, where isotopic compositions suggest mixing with evaporated surface water. The observed evaporation-driven isotopic enrichment in ponds and rivers, contrasted with the relatively stable isotopic signature of deeper groundwater, underscores the heterogeneity in recharge mechanisms and the potential vulnerability of shallow aquifers to seasonal fluctuations.

The study's findings underscore the urgent need for targeted water resource management strategies to address both quantity- and quality-related challenges. To mitigate groundwater depletion and contamination risks, policymakers must prioritize sustainable groundwater recharge initiatives, including rainwater harvesting, managed aquifer recharge (MAR), and stringent pollution control measures. Additionally, the implemen-

tation of long-term hydrological monitoring programs is essential to track spatiotemporal variations in water chemistry and isotopic composition, enabling more informed decision-making.

Future research should focus on quantifying recharge rates, delineating pollution sources, and assessing the socio-economic implications of water stress. By integrating scientific research with policy frameworks, fostering multi-stakeholder collaboration, and engaging local communities in conservation efforts, a more resilient and sustainable water management system can be established for Raipur and its surrounding regions.

Author Contributions: Conceptualization, D.J.; Methodology, D.J. and M.S.; Software, M.S.; Formal analysis, R.D.D. and V.P.; Investigation, M.S.; Resources, D.J.; Data curation, M.S., R.D.D. and V.P.; Writing—original draft, M.S.; Writing—review & editing, D.J.; Supervision, D.J.; Project administration, D.J.; Funding acquisition, D.J. All authors have read and agreed to the published version of the manuscript.

Funding: This research project is sponsored by the Science and Engineering Research Board (SERB), a division of the Department of Science and Technology, Government of India, under the Empowerment and Equity Opportunities for Excellence in Science (EMEQ) initiative (File Number: EEQ/2021/000945).

Data Availability Statement: Data is contained within the article.

Acknowledgments: We sincerely thank the SERB for its financial support and encouragement. We also thank the National Institute of Technology Raipur, Chhattisgarh, India for providing the necessary infrastructural support.

Conflicts of Interest: The authors declare no conflict of interest.

References

1. Appleyard, S. The Impact of Urban Development on Recharge and Groundwater Quality in a Coastal Aquifer Near Perth, Western Australia. *Hydrogeol. J.* **1995**, *3*, 65–75. [CrossRef]
2. Davila, P.R.A.; Leon, G.D.H.; Schuth, C. Urban impacts analysis on hydrochemical and hydrogeological evolution of groundwater in shallow aquifer Linares, Mexico. *Environ. Earth Sci.* **2012**, *66*, 1871–1880. [CrossRef]
3. Dimitriou, E.; Moussoulis, E. Land use change scenarios and associated groundwater impacts in a protected peri-urban area. *Environ. Earth Sci.* **2011**, *64*, 471–482. [CrossRef]
4. Krishan, G.; Singh, S.; Thayyen, R.J.; Ghosh, N.C.; Rai, S.P.; Arora, M. Understanding river–subsurface water interactions in upper Ganga basin, India. *Int. J. River Basin Manag.* **2020**, *18*, 243253. [CrossRef]
5. Mohrlok, U.; Wolf, L.; Klinger, J. Quantification of infiltration processes in urban areas by accounting for spatial parameter variability. *J. Soils Sediments* **2008**, *8*, 34–42. [CrossRef]
6. Mukherjee, A.; Babu, S.S.; Ghosh, S. Thinking about water and air to attain sustainable development goals during times of COVID-19 pandemic. *J. Earth Syst. Sci.* **2020**, *129*, 180. [CrossRef]
7. Park, S.; Kim, S.; Yun, S.; Kim, S.; Chae, G.; Yu, S.; Kim, S.; Kim, Y. Effects of land use on the spatial distribution of trace metals and volatile organic compounds in urban groundwater, Seoul, Korea. *Environ. Geol.* **2005**, *48*, 1116–1131. [CrossRef]
8. Scanlon, B.R.; Reedy, C.R.; Stonestrom, A.D.; Prudic, E.D.; Dennehy, F.K. Impact of land use and land cover change on groundwater recharge and quality in the southwestern US. *Glob. Change Biol.* **2005**, *11*, 1577–1593. [CrossRef]
9. Shi, X.; Jiang, S.; Xu, H.; Jiang, F.; He, Z.; Wu, J. The effects of artificial recharge of groundwater on controlling land subsidence and its influence on groundwater quality and aquifer energy storage in Shanghai, China. *Environ. Earth Sci.* **2016**, *75*, 195. [CrossRef]
10. Yan, B.; Xiao, C.; Liang, X.L.; Fang, Z. Arab J Impacts of urban land use on nitrate contamination in groundwater, Jilin City, Northeast China. *Arab. J. Geosci.* **2016**, *9*, 105. [CrossRef]
11. Duttagupta, S.; Mukherjee, A.; Bhattacharya, A.; Bhattacharya, J. Wide exposure of persistent organic pollutants (PoPs) in natural waters and sediments of the densely populated Western Bengal basin, India. *Sci. Total Environ.* **2020**, *717*, 137187. [CrossRef]
12. Duttagupta, S.; Mukherjee, A.; Das, K.; Dutta, A.; Bhattacharya, A.; Bhattacharya, J. Groundwater vulnerability to pesticide pollution assessment in the alluvial aquifer of Western Bengal basin, India using overlay and index method. *Geochemistry* **2020**, *80*, 125601. [CrossRef]
13. Gourcy, L.L.; Groening, M.; Aggarwal, P.K. Stable oxygen and hydrogen isotopes in precipitation. In *Isotopes in the Water Cycle*; Springer: Dordrecht, The Netherlands, 2005; pp. 39–51.

14. Shamsudduha, M. Groundwater resilience to human development and climate change in South Asia. In *Global Water Forum (GWF) Discussion Paper*; Global Water Forum: Canberra, Australia, 2013; Volume 1332.
15. Yun, P.; Huili, G.; Demin, Z.; Xiaojuan, L.; Nobukazu, N. Impact of land use change on groundwater recharge in Guishui River Basin, China. *Chin. Geogr. Sci.* **2011**, *21*, 734–743.
16. Cosgrove, D.M.; Johnson, G.S. Aquifer management zones based on simulated surface-water response functions. *J. Water Resour. Plan. Manag.* **2005**, *131*, 89–100. [CrossRef]
17. Das, P.; Mukherjee, A.; Lapworth, D.J.; Das, K.; Bhaumik, S.; Layek, M.K.; Shaw, A.; Smith, M.; Sengupta, P.; MacDonald, A.M.; et al. Quantifying the dynamics of sub-daily to seasonal hydrological interactions of Ganges river with groundwater in a densely populated city: Implications to vulnerability of drinking water sources. *J. Environ. Manag.* **2021**, *288*, 11238. [CrossRef]
18. Lewandowski, J.; Lischeid, G.; Nützmann, G. Drivers of water level fluctuations and hydrological exchange between groundwater and surface water at the lowland River Spree (Germany): Field study and statistical analyses. *Hydrol. Process.* **2009**, *23*, 2117–2128. [CrossRef]
19. MacDonald, A.M.; Bonsor, H.C.; Ahmed, K.M.; Burgess, W.G.; Basharat, M.; Calow, R.C.; Dixit, A.; Foster, S.S.D.; Gopal, K.; Lapworth, D.J.; et al. Groundwater quality and depletion in the Indo-Gangetic Basin mapped from in situ observations. *Nat. Geosci.* **2016**, *9*, 762–766. [CrossRef]
20. Maurya, A.S.; Shah, M.; Deshpande, R.D.; Bhardwaj, R.M.; Prasad, A.; Gupta, S.K. Hydrograph separation and precipitation source identification using stable water isotopes and conductivity: River Ganga at Himalayan foothills. *Hydrol. Process.* **2011**, *25*, 1521–1530. [CrossRef]
21. Mukherjee, A. (Ed.) *Groundwater of South Asia*; Springer: Berlin/Heidelberg, Germany, 2018.
22. Mukherjee, A.; Fryar, A.E.; Rowe, H.D. Regional-scale stable isotopic signatures of recharge and deep groundwater in the arsenic affected areas of West Bengal, India. *J. Hydrol.* **2007**, *334*, 151–161. [CrossRef]
23. Mukherjee, A.; Saha, D.; Harvey, C.F.; Taylor, R.G.; Ahmed, K.M.; Bhanja, S.N. Groundwater systems of the Indian sub-continent. *J. Hydrol. Reg. Stud.* **2015**, *4*, 1–14. [CrossRef]
24. Rosenshein, J.S. Region 18, Alluvial Valleys. In *Hydrogeology*; The Geological Society of North America: Boulder, CO, USA, 1988; pp. 165–175.
25. Blanco-Coronas, A.M.; López-Chicano, M.; Calvache, M.L.; Benavente, J.; Duque, C. Groundwater-Surface Water Interactions in "La Charca de Suárez" Wetlands, Spain. *Water* **2020**, *12*, 344. [CrossRef]
26. Wehrhahn, R.; Bercht, A.L.; Krause, C.L.; Azzam, R.; Kluge, C.L.; Strohschön, R.; Wiethoff, K.; Baier, K. Urban restructuring and social and water-related vulnerability in mega-cities—The example of the urban village of Xincún, Guangzhou (China). In *Die Erde. Zeitschrift der Gesellschaft für Erdkunde zu Berlin*; Geographical Society of Berlin: Berlin, Germany, 2008; Volume 139, pp. 227–249.
27. Wiethoff, K.; Baier, K. Megacities Areas in Transition. Abandoned Sites as an Expression of a Continuously Changing mega-urban landscape. In *Proceedings of the Megacities—Interactions Between Land Use and Water Management—Mitteilungen zur Ingenieurgeologie und Hydrogeologie, Guangzhou, China, 25–26 November 2009*; Baier, K., Strohschön, R., Eds.; RWTH Publications: Aachen, Germany, 2009; Volume 99, pp. 83–92.
28. Gangwar, S. Water Resource of India: From Distribution to Management. *Int. J. Inf. Comput. Technol.* **2013**, *3*, 845–850.
29. Joshi, S.K.; Rai, S.P.; Sinha, R.; Gupta, S.; Densmore, A.L.; Rawat, Y.S.; Shekhar, S. Tracing groundwater recharge sources in the northwestern Indian alluvial aquifer using water isotopes (δ18O, δ2H and 3H). *J. Hydrol.* **2018**, *559*, 835–847.
30. Bhat, N.A.; Jeelani, G. Quantification of groundwater–surface water interactions using environmental isotopes: A case study of Bringi Watershed, Kashmir Himalayas, India. *J. Earth Syst. Sci.* **2018**, *127*, 63. [CrossRef]
31. Kumar, S.K.; Babu, S.H.; Rao, P.E.; Selvakumar, S.; Thivya, C.; Muralidharan, S.; Jeyabal, G. Evaluation of water quality and hydrogeochemistry of surface and groundwater, Tiruvallur District, Tamil Nadu, India. *Appl. Water Sci.* **2017**, *7*, 2533–2544. [CrossRef]
32. Maharjan, M.; Donovan, J.J. Groundwater response to serial stream stage fluctuations in shallow unconfined alluvial aquifers along a regulated stream (West Virginia, USA). *Hydrogeol. J.* **2016**, *24*, 2003–2015. [CrossRef]
33. Jat, M.K.; Khare, D.; Garg, P.K. Urbanization and its impact on groundwater: A remote sensing and GIS-based assessment approach. *Environmentalist* **2009**, *29*, 17–32. [CrossRef]
34. Krishan, G.; Singh, S.; Sharma, A.; Sandhu, C.; Kumar, S.; Kumar, C.P.; Gurjar, S. Assessment of river Yamuna and groundwater interaction using isotopes in Agra and Mathura area of Uttar Pradesh, India. *Int. J. Hydrol.* **2017**, *1*, 86–89. [CrossRef]
35. Madhuri, R.; Verma, M.K.; Tripathi, R.K. Impact of Urbanisation on water resources in Raipur city using GIS and Remote Sensing. *Int. J. Earth Sci. Eng.* **2012**, *5*, 1815–1819.
36. Misra, A.K. Impact of Urbanization on the Hydrology of Ganga Basin (India). *Water Resour. Manag.* **2011**, *25*, 705–719. [CrossRef]
37. Pandit, M.K.; Bhardwaj, V.; Pareek, N. Urbanization impact on hydrogeological regime in Jaipur Urban Block: A rapidly growing urban center in NW India. *Environmentalist* **2009**, *29*, 341–347. [CrossRef]

38. Pradeep, K.N.; Jivesh, A.T.; Biranchi, N.D.; Arun, N.T. Impact of urbanization on the groundwater regime in a fast growing city in central India. *Environ. Monit. Assess.* **2008**, *146*, 339–373. [CrossRef]
39. Rao, N.P.; Prasad, K.M.; Madhusudhan, B.J.; Krishna, V.S.R.; Anand, A.V.S.S.; Madhnure, P. Impact of Urbanization on Groundwater Quality in Vijayawada Urban Agglomeration, the New Capital Region of Andhra Pradesh, India—A Baseline Study. *J. Geol. Soc. India* **2016**, *87*, 539–552.
40. Saumya, S.; Samaddar, A.B.; Srivastava, R.K.; Pandey, H.K. Ground Water Recharge in Urban Areas—Experience of Rain Water Harvesting. *J. Geol. Soc. India* **2014**, *83*, 295–302.
41. Sharma, S.; Bharat, A.; Das, M.V. Study of Variations in Urban and Hydrological Components in Process of Urbanization. *Int. J. Eng. Res.* **2013**, *2*, 203–207.
42. Singh, A.; Srivastav, K.S.; Kumar, S.; Chakrapani, J.G. A modified DRASTIC model (DRASTICA) for assessment of groundwater vulnerability to pollution in an urbanized environment in Lucknow, India. *Environ. Earth Sci.* **2015**, *74*, 5475–5490. [CrossRef]
43. Wakode, H.B.; Baier, K.; Jha, R.; Ahmed, S.; Azzam, R. Assessment of Impact of Urbanization on Groundwater Resources using GIS Techniques—Case Study of Hyderabad, India. *Int. J. Environ. Res.* **2014**, *8*, 1145–1158.
44. Das, S.; Nag, K.S. Application of multivariate statistical analysis concepts for assessment of hydrogeochemistry of groundwater—A study in Suri I and II blocks of Birbhum District, West Bengal, India. *Appl. Water Sci.* **2017**, *7*, 873–888. [CrossRef]
45. Khan, N.M.M.S.; Kumar, R.A. Interpretation of groundwater quality using correlation and linear regression analysis from tiruchengode taluk, namakkal district, tamilnadu, India. *J. Chem. Pharm. Res.* **2012**, *4*, 4514–4521.
46. Shroff, P.; Vashi, T.R.; Champaneri, A.V.; Patel, K.K. Correlation study among water quality parameters of groundwater of valsad district of south Gujarat (India). *J. Fund. Appl. Sci.* **2015**, *7*, 340–349.
47. Kothari, V.; Vij, S.; Sharma, K.S.; Gupta, N. Correlation of various water quality parameters and water quality index of districts of Uttarakhand. *Environ. Sustain. Indic.* **2020**, *9*, 100093. [CrossRef]
48. Bhat, S.A.; Meraj, G.; Yaseen, S.; Pandit, A.K. Statistical assessment of water quality parameters for pollution source identification in sukhnag stream: An inflow stream of lake wular (ramsar site), kashmir himalaya. *J. Ecosyst.* **2014**, *2014*, 898054. [CrossRef]
49. Doza, B.; Islam, S.D.-U.; Rume, T.; Quraishi, S.B.; Rahman, M.S.; Bhuiyan, M.A.H. Groundwater quality and human health risk assessment for safe and sustainable water supply of Dhaka City dwellers in Bangladesh. *Groundw. Sustain. Dev.* **2020**, *10*, 100374. [CrossRef]
50. Tokatli, C.; Kose, E.; Cicek, A.; Emiroglu, O.; Bastatli, Y. Use of cluster Analysis to evaluate surface water quality: An application from downstream of meric river basin (edirne, Turkey). *Int. J. Adv. Sci. Eng. Technol.* **2015**, *3*, 33–35.

Disclaimer/Publisher's Note: The statements, opinions and data contained in all publications are solely those of the individual author(s) and contributor(s) and not of MDPI and/or the editor(s). MDPI and/or the editor(s) disclaim responsibility for any injury to people or property resulting from any ideas, methods, instructions or products referred to in the content.